Membrane Transport.

Lecture One: Structure and Function of Membranes.

source: Gennis, RB 1989 Biomembranes. Molecular Structure and Function. Springer-Verlag. Chapters One and Two.

<u>definitions</u> : Membranes are....

i) structural entities that compartmentalize cellular functions.

ii) used to isolate the functional and structural aspects of life from the external environment.

iii) the location of initial steps in signal transduction, mediating cellular responses to external stimuli.

<u>composition</u>

LIPIDS → phospholipids
LIPIDS → sterols

PROTEINS → intrinsic
PROTEINS → extrinsic.

examples of i) membrane architecture
ii) procaryotic membrane structure
iii) eucaryotic membrane structure.

Transparency 11
Figure 5–5, page 105
Model of cell membrane

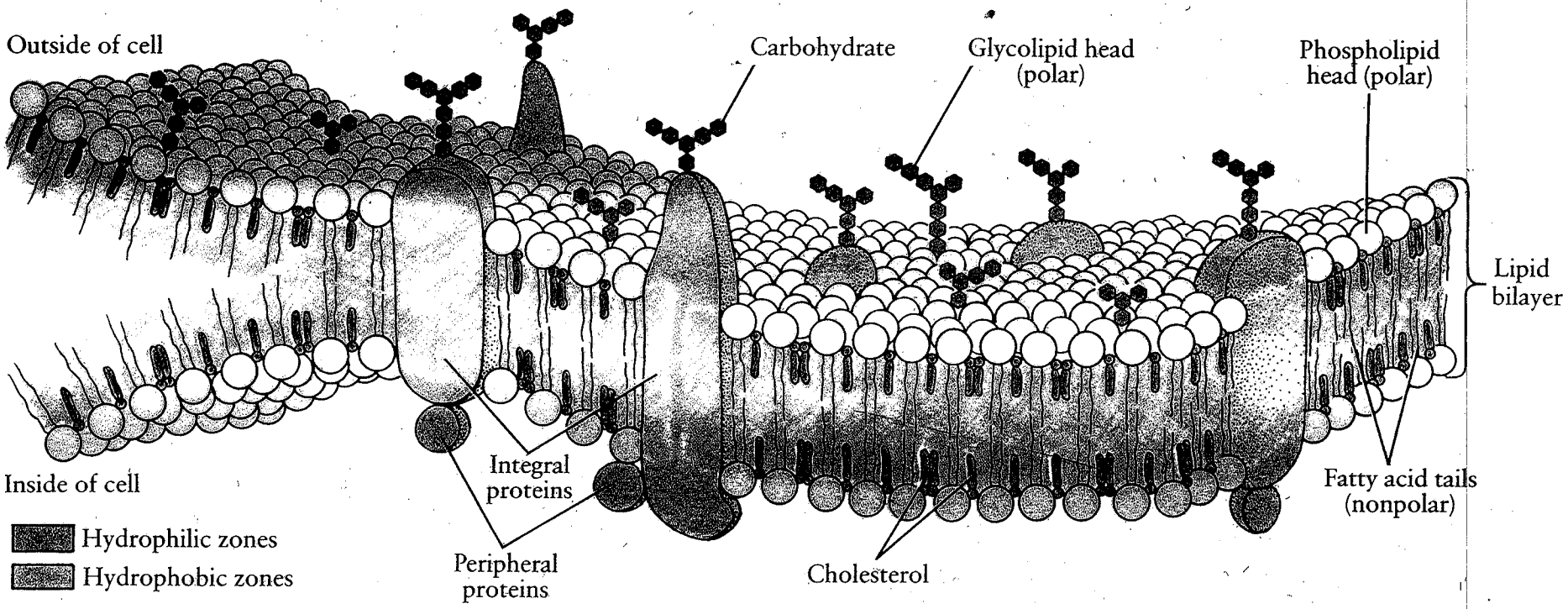

Bacterial cell (E. coli)
Figure 4–8, page 18
Transparency 2

Transparency 6

Figure 4–9, page 92

Photosynthetic prokaryote *(Anabaena)*

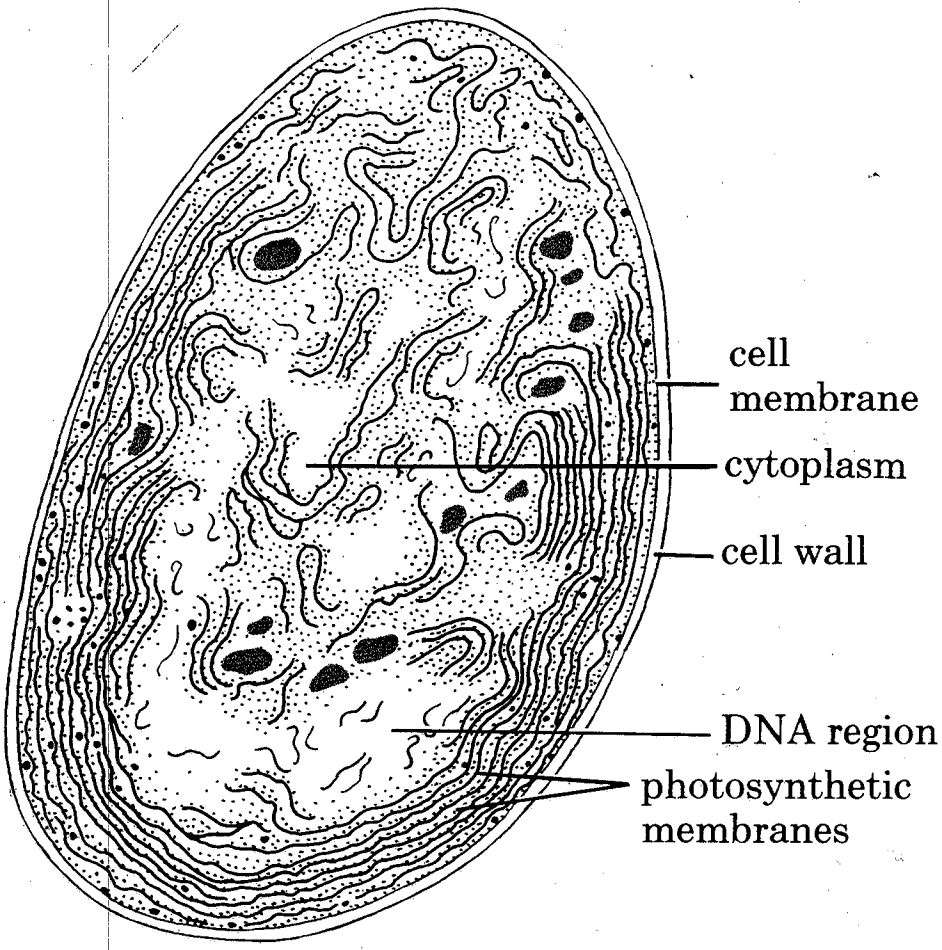

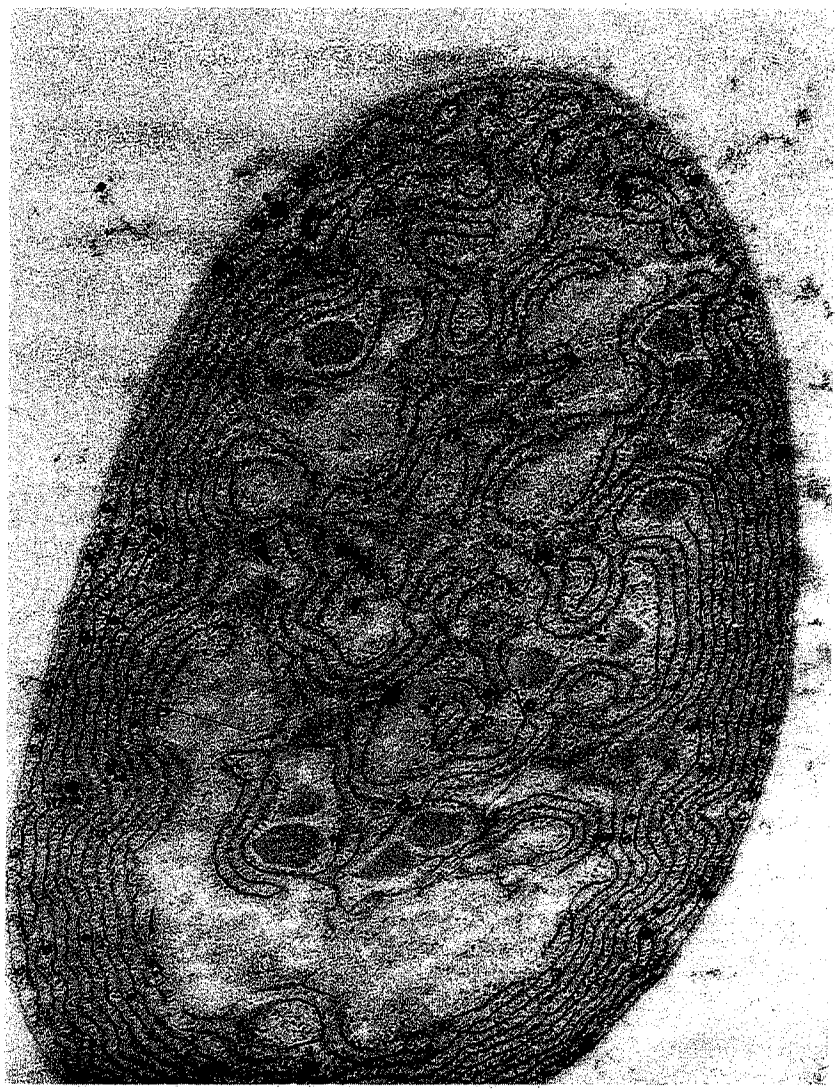

Transparency 7

Figure 4–10, page 92

Photosynthetic eukaryote *(Chlamydomonas)*

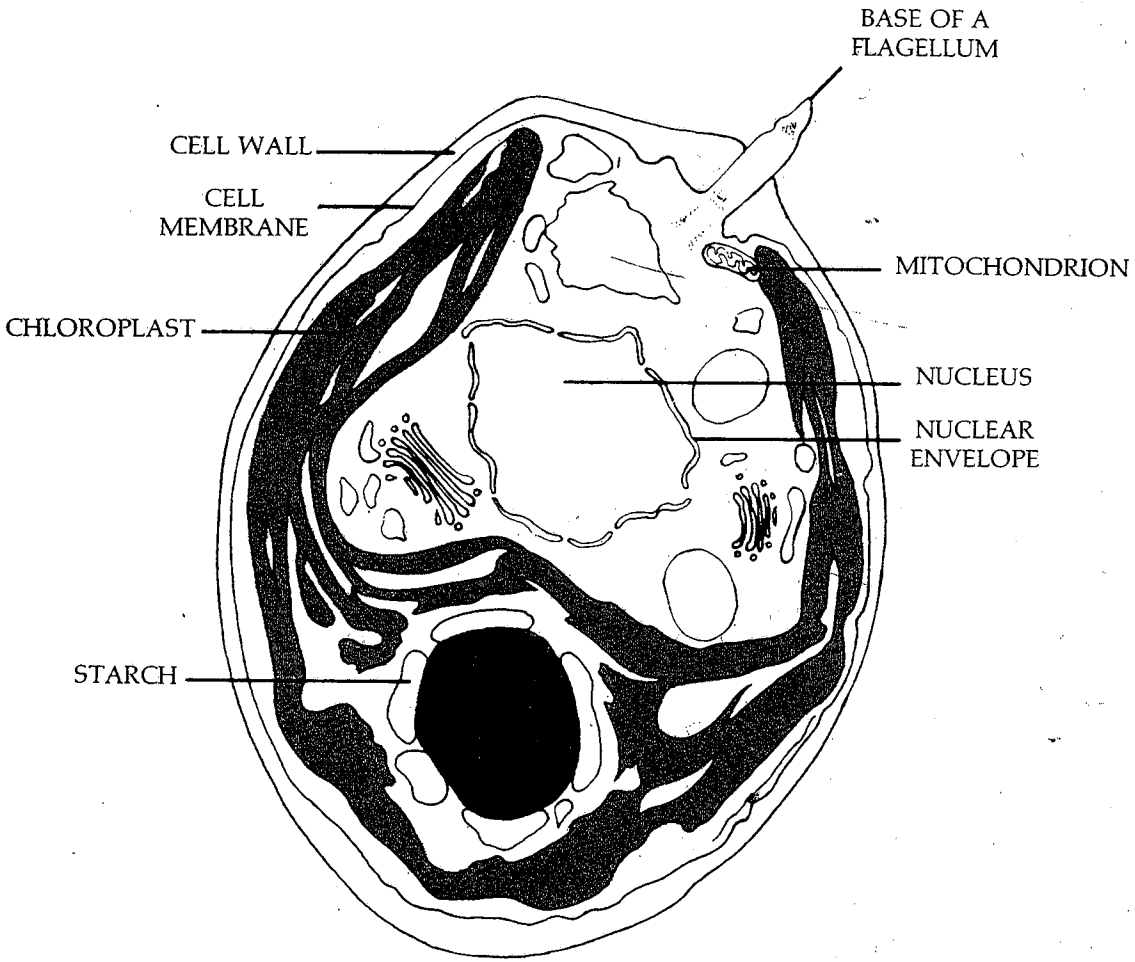

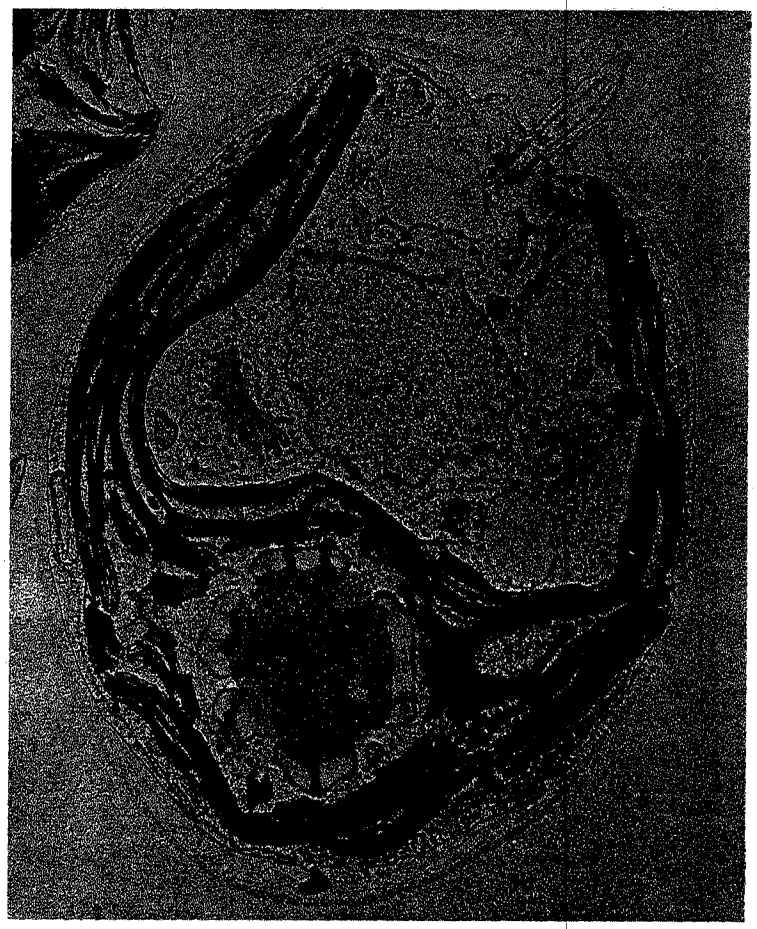

Membranous Dynamics

2484 Biophysical Journal Volume 81 November 2001 2484-2494

Dynamical Properties of a Hydrated Lipid Bilayer from a Multinanosecond Molecular Dynamics Simulation

Preston B. Moore, Carlos F. Lopez, and Michael L. Klein
Center for Molecular Modeling and Department of Chemistry, University of Pennsylvania, Philadelphia, Pennsylvania 19104 USA

FIGURE 1 The chemical bonding representation of the DMPC (dimiristoylphosphatidylcholine) molecule. Carbon atom labeling is referenced throughout the text. The head group Zwitterion dipole is indicated by the P-N vector.

Source: Preston B. Moore, Carlos F. Lopez, and Michael L. Klein (2001) Dynamical Properties of a Hydrated Lipid Bilayer from a Multinanosecond Molecular Dynamics Simulation. Biophys J 81:2484-2494.

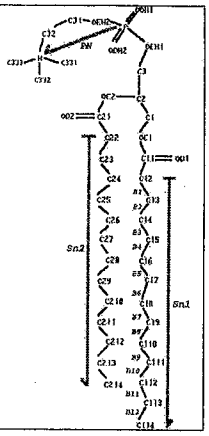

FIGURE 8 Ten superimposed structure snapshots for different time intervals (left to right: 100 ps, 1 ns, and 10 ns).

Source: Preston B. Moore, Carlos F. Lopez, and Michael L. Klein (2001) Dynamical Properties of a Hydrated Lipid Bilayer from a Multinanosecond Molecular Dynamics Simulation. Biophys J 81:2484-2494.

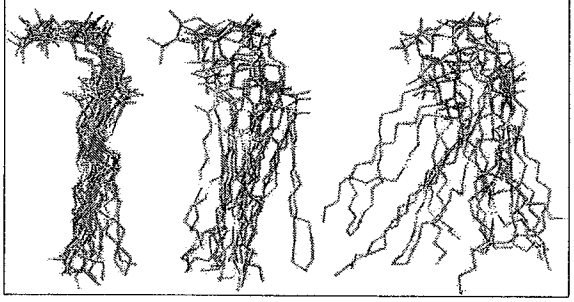

FIGURE 1 Snapshot of a fully equilibrated hydrated POPC (palmitoyl-oleyl phosphatidylcholine) bilayer. Water molecules are color-coded red (H) and white (O). Lipid methyls and methylenes are color-coded gray. C=C atoms are color-coded cyan. Headgroup P atoms are yellow, and headgroup N atoms are blue.

Source: S. W. Chiu, Eric Jakobsson, Shankar Subramaniam, and H. Larry Scott (1999) Combined Monte Carlo and Molecular Dynamics Simulation of Fully Hydrated Dioleyl and Palmitoyl-oleyl Phosphatidylcholine Lipid Bilayers. Biophys J 77:2462-2469

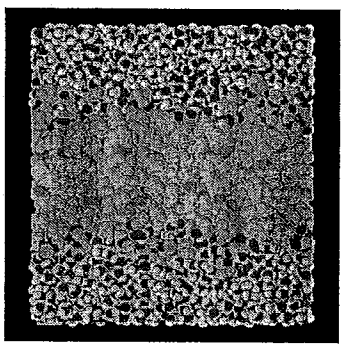

Membranous Dynamics

Rapid flexing of the phospholipid acyl chains churns the membrane, but the hydrophobicity of the acyl chains maintains the bilayer barrier between aqueous compartments.

Membranous Cells

Organellar relationships in the Golgi region of the pancreatic beta cell line, HIT-T15, visualized by high resolution electron tomography

Brad J. Marsh*, David N. Mastronarde*, Karolyn F. Buttle†, Kathryn E. Howell‡, and J. Richard McIntosh*§

*Boulder Laboratory for 3-D Fine Structure, Department of Molecular, Cellular and Developmental Biology, University of Colorado, Boulder, CO 80309; †Resource for the Visualization of Biological Complexity, Wadsworth Center, Albany, NY 12201; and ‡Department of Cellular and Structural Biology, University of Colorado School of Medicine, Denver, CO 80262

This contribution is part of the special series of Inaugural Articles by members of the National Academy of Sciences elected on May 2, 2000

Contributed by J. Richard McIntosh, December 29, 2000

6

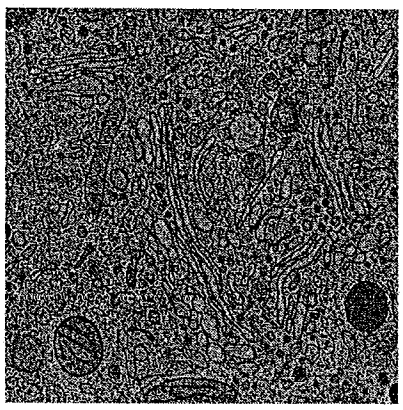

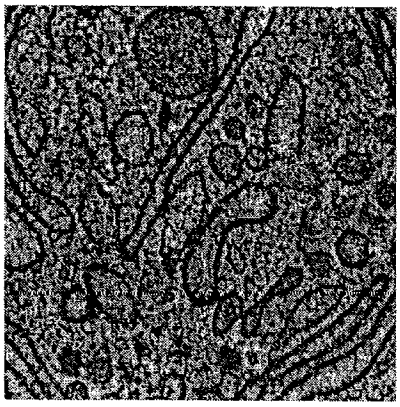

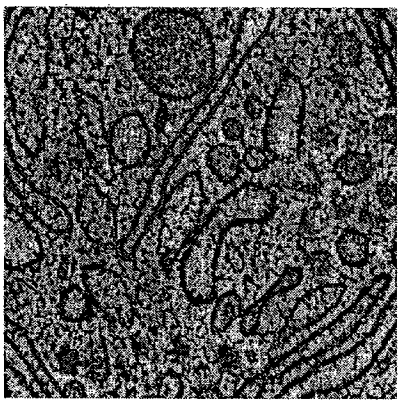

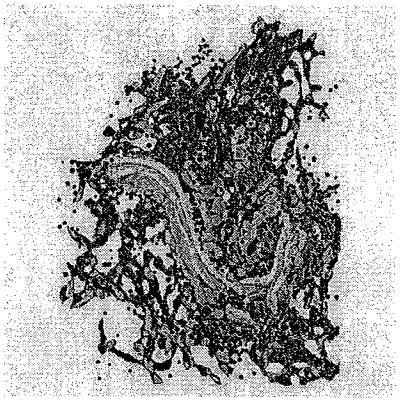

Membranous Cells

Serial sectioning and tomography reveal clearly that eucaryotic cells contain a three-dimensional array of diverse membrane compartments that function in cellular metabolism, growth and division.

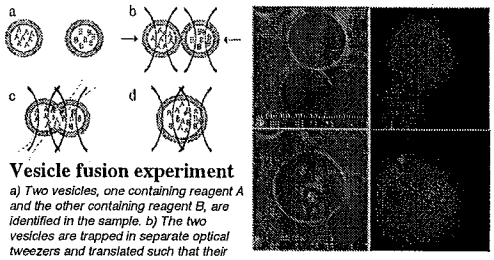

Vesicle fusion experiment

a) Two vesicles, one containing reagent A and the other containing reagent B, are identified in the sample. b) The two vesicles are trapped in separate optical tweezers and translated such that their membranes come into contact. c) Fusion is initiated by a pulsed UV laser, which disrupts the membranes of both vesicles at the contact point. d) The membranes repair spontaneously by forming one larger vesicle in which reagents A and B mix and react.

source: http://physics.nist.gov/Divisions/Div842/Gp4/Tweezers/research.html

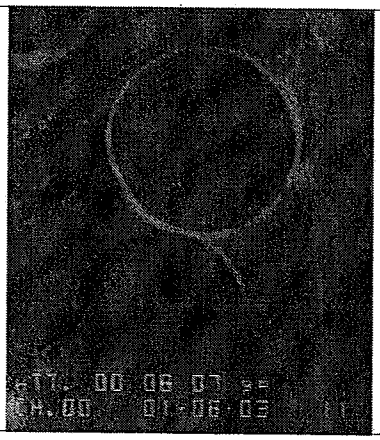

Spontaneous formation of 'hyphal' morphology from hydrating phospholipids

The lipids were dried onto glass, then hydrated by adding a buffered solution. Over 60 minutes, spontaneous structures appear, from spherical to cyclindrical in shape.

source: Dr. Natalia N. Levina, York-Biology, Toronto, Canada

8

LIPIDS → phospholipids.

general structure

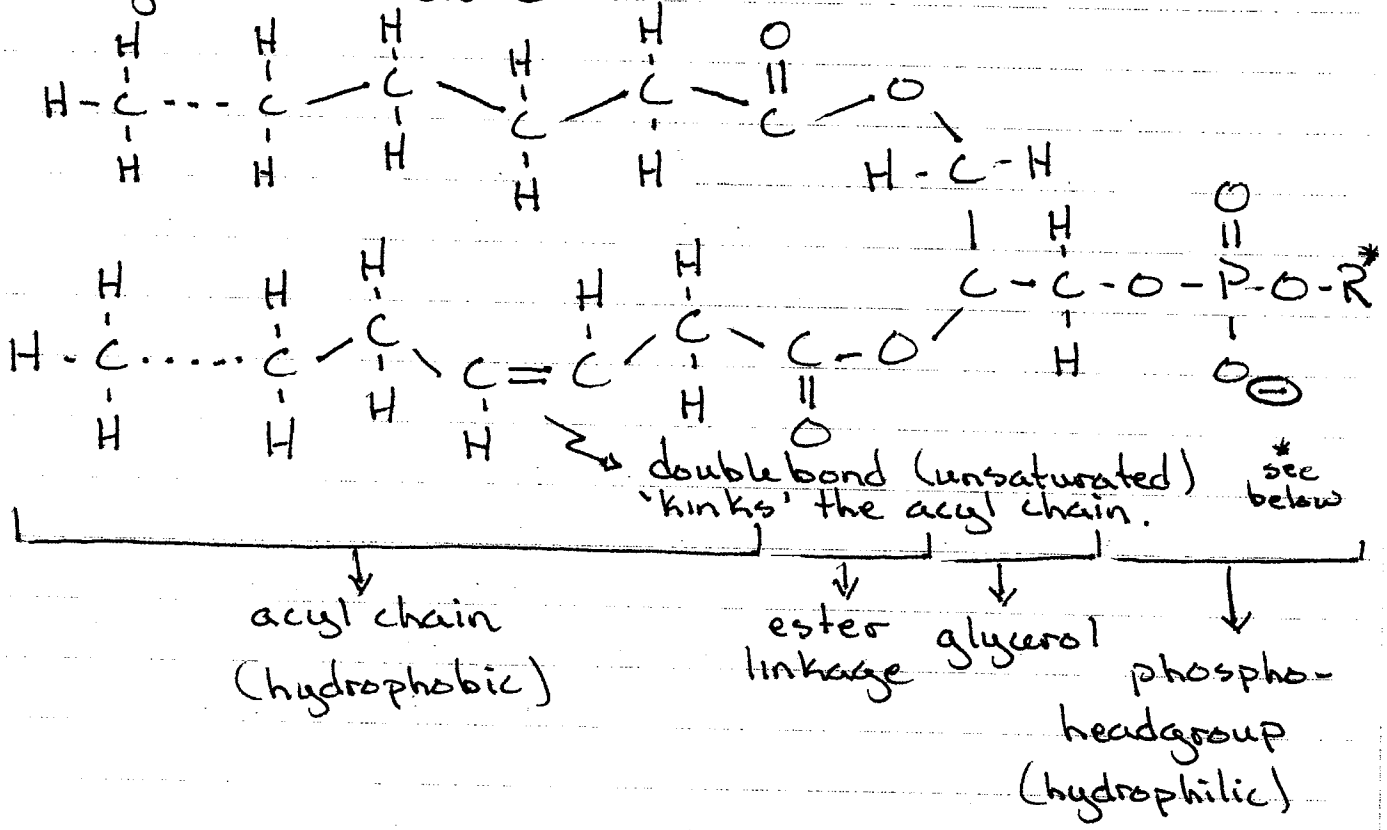

acyl chain length : 12 - 22 carbons long with 0 - 4 unsaturated bonds.

headgroups:

R = H (phosphatidic acid - PA)

R = $-CH_2-CH_2-N^+-(CH_3)_3$ (phosphatidylcholine - PC)

R = $-CH_2-CH_2-NH_3^+$ (phosphatidylethanolamine - PE)

R = $-CH_2-\underset{\underset{COO^-}{|}}{CH}-NH_3^+$ (phosphatidylserine - PS)

[R = inositol (phosphatidylinositol - PI)

Phospholipid head group properties.

By comparison with the acyl chain, the phosphoryl head group is highly polar, very hydrophilic. This is due to the -ve charge on the phosphate as well as other polar or charged groups.

Thus, phosphatidylcholine

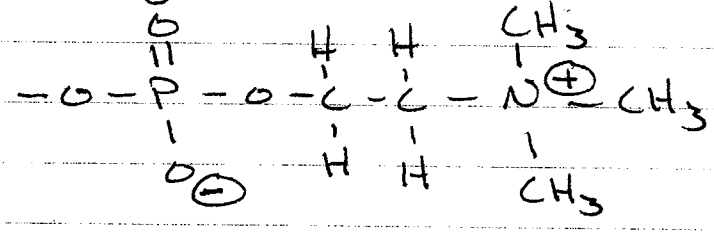

and phosphatidylethanolamine

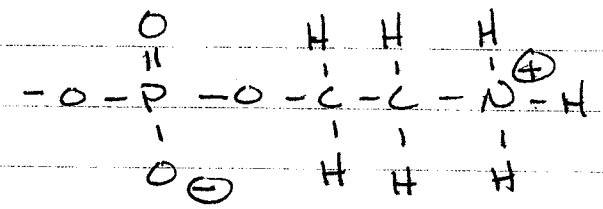

nb note the difference in the bulkiness of the head-group.

are zwitterions (charged, but net charge is zero

while phosphatidylserine

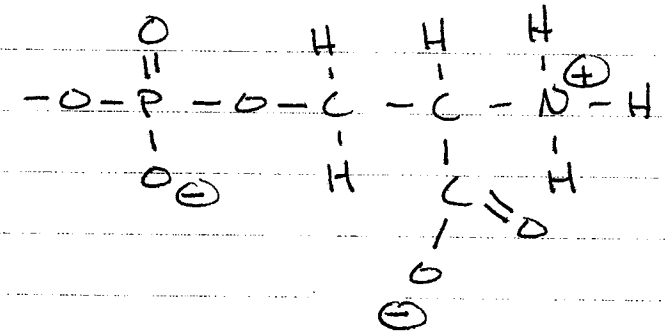

has a net -ve charge.

Of all the usual phospholipids in biological membranes, phosphatidylserine (PS) is notable for its assymetric location in the membrane.

In plasma membrane, it is preferentially located on the inner leaflet of the membrane[1]. It has been implicated as a component in Ca^{2+}-mediated fusion of adjacent membranes – an absolute requirement in secretion, including neurotransmitter release.

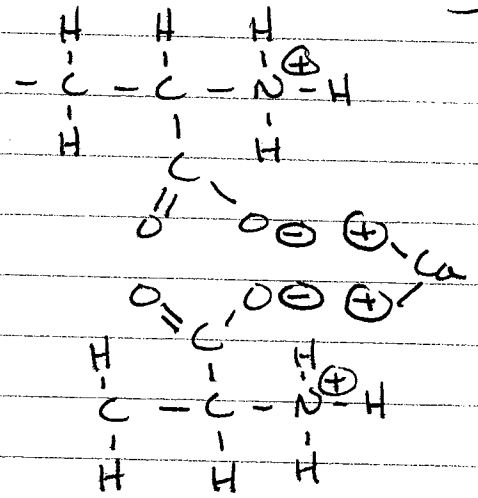

ionic bonds between the two -ve carboxylts and the two +ve charges of calcium result in cross-linking of PS molecules in the membrane.

1) J.A.F. Op den Kamp 1979 Lipid assymetry in membranes, Ann. Rev. Biochem. 48 47-71.

The result of cross-linking, if we look 'down' on the face of the membrane:

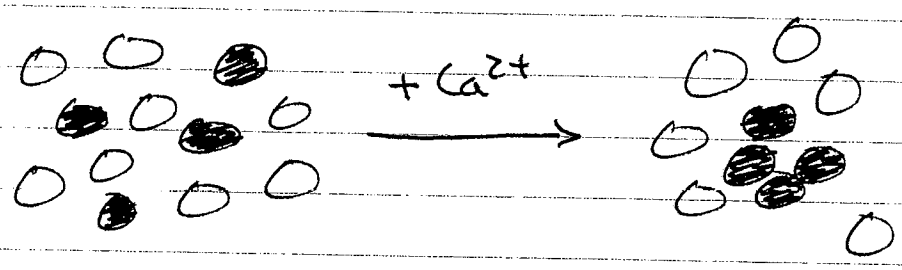

is lateral phase separation

a 'sideways' view:

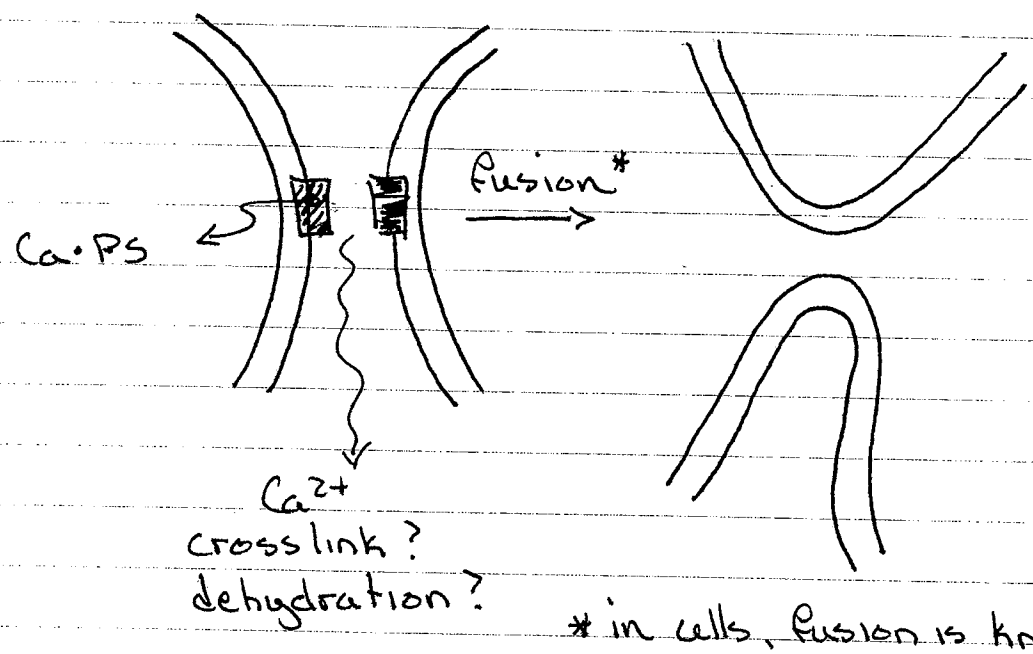

* in cells, fusion is known to be protein-mediated, but also appears to require PS and Ca^{2+}

One other phospholipid, normally present at low concentrations, plays a direct role in signal transduction: phosphatidylinositol diphosphate. (PIP_2)

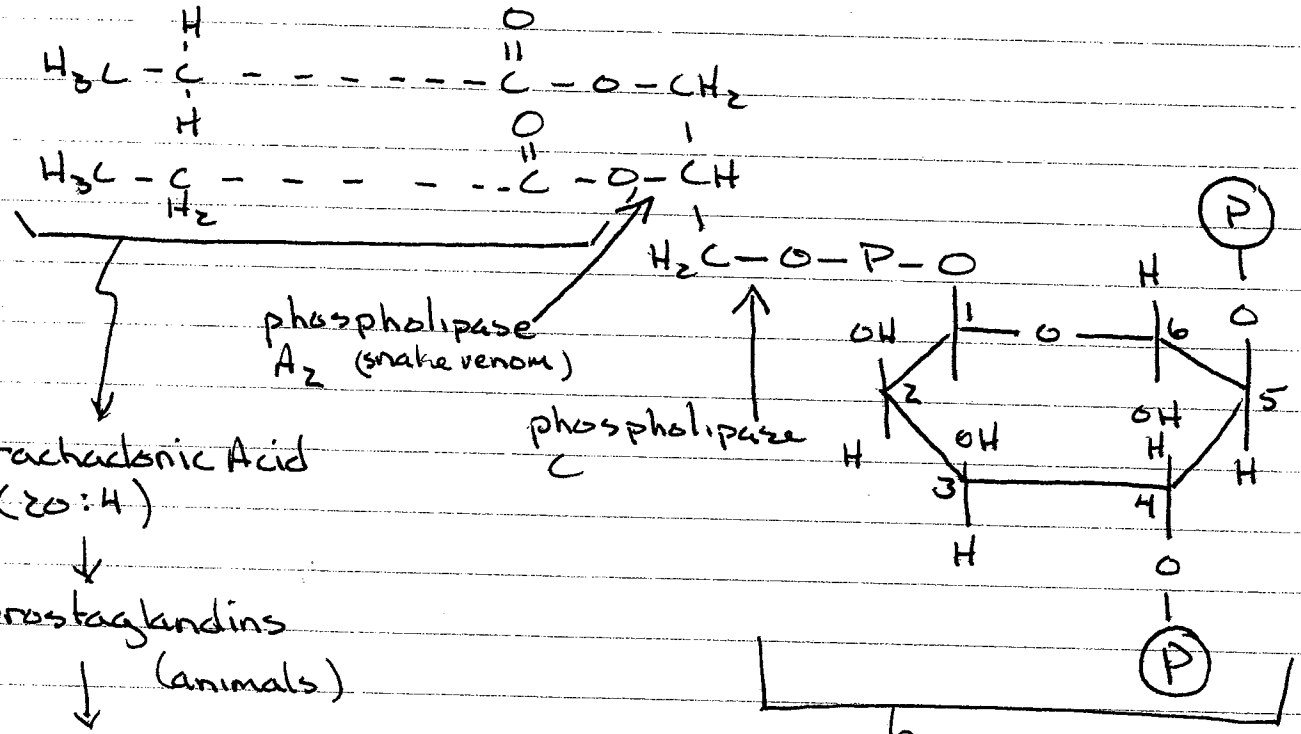

PIP_2 is cleaved by phospholipase C, releasing inositol-1,4,5-trisphosphate. Phospholipase A_2 (diacyl glycerol lipase) cleaves the diacylglycerol to yield arachidonic acid. Diacylglycerol itself is known to activate protein kinase C. So, varying cleavages of PIP_3 result in three second messengers.

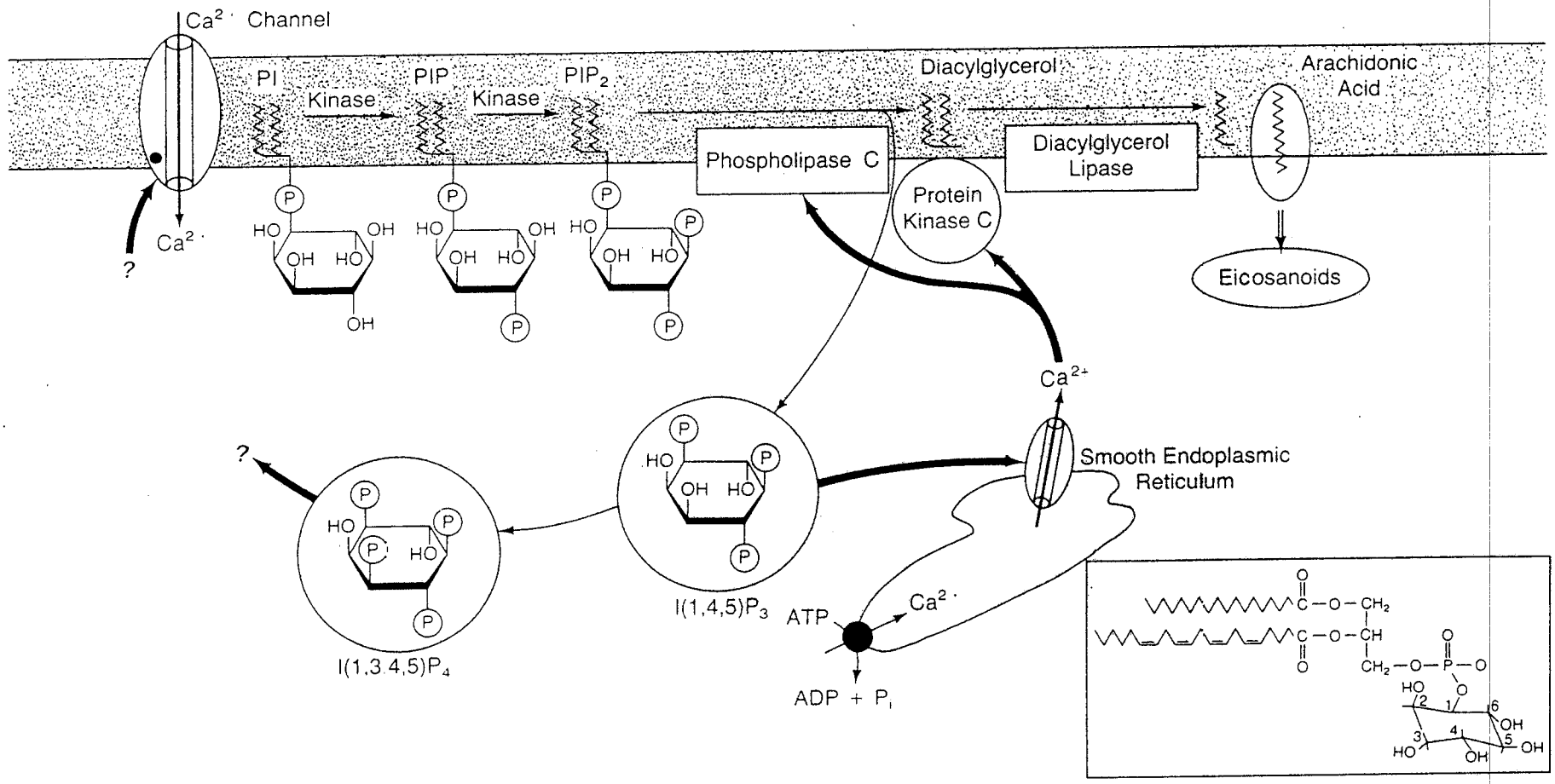

Figure 9.16. Representation of the generation of second messengers by the agonist-induced breakdown of phosphatidylinositol (PI). The system is activated in many cells by a G protein, which stimulates the PI-specific phospholipase C. IP_3 is known to result in the mobilization of Ca^{2+} sequestered in the endoplasmic reticulum, and it is possible that IP_3 and IP_4 act together to allow Ca^{2+} to enter the cell across the plasma membrane. The inset shows the structure of a typical PI species, enriched in stearate (*sn*-1) and arachidonate (*sn*-2). See text for details.

There are other lipids which are very important in the composition of membranes. I want to highlight some examples.

cardiolipin is a major lipid in mitochondrial membranes. It is a diphosphatidylglycerol, essentially a dimeric phospholipid.

Abbreviated structure:

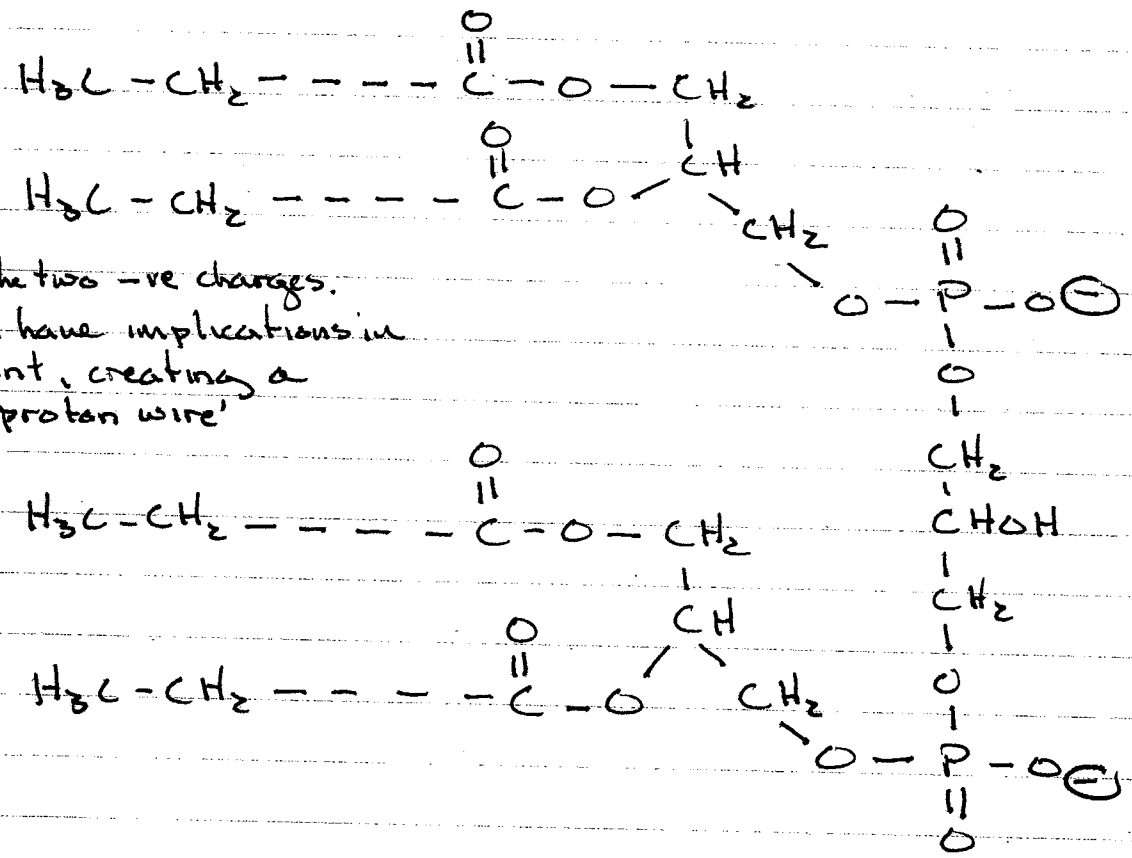

nb note the two -ve charges. This could have implications in H^+ movement, creating a surface 'proton wire'

It composes 18% of the mitochondrial lipid and about 1% in all other organellar membranes.

Note that mitochondria are highly specialized respiratory engines. The presence of cardiolipin implies specialized membrane architexture requirements.

Cardiolipin (from *E. coli*, but a common lipid in mitochondrial membranes of eukaryotes)

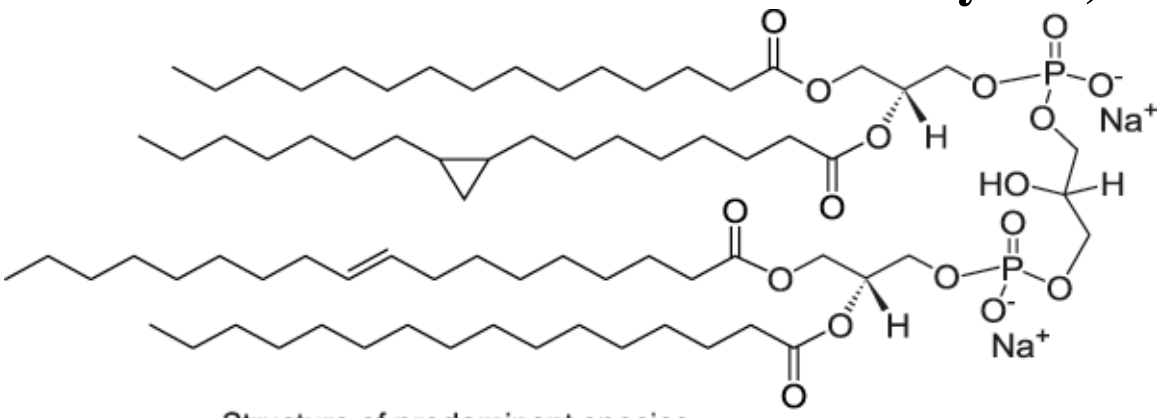

Structure of predominant species

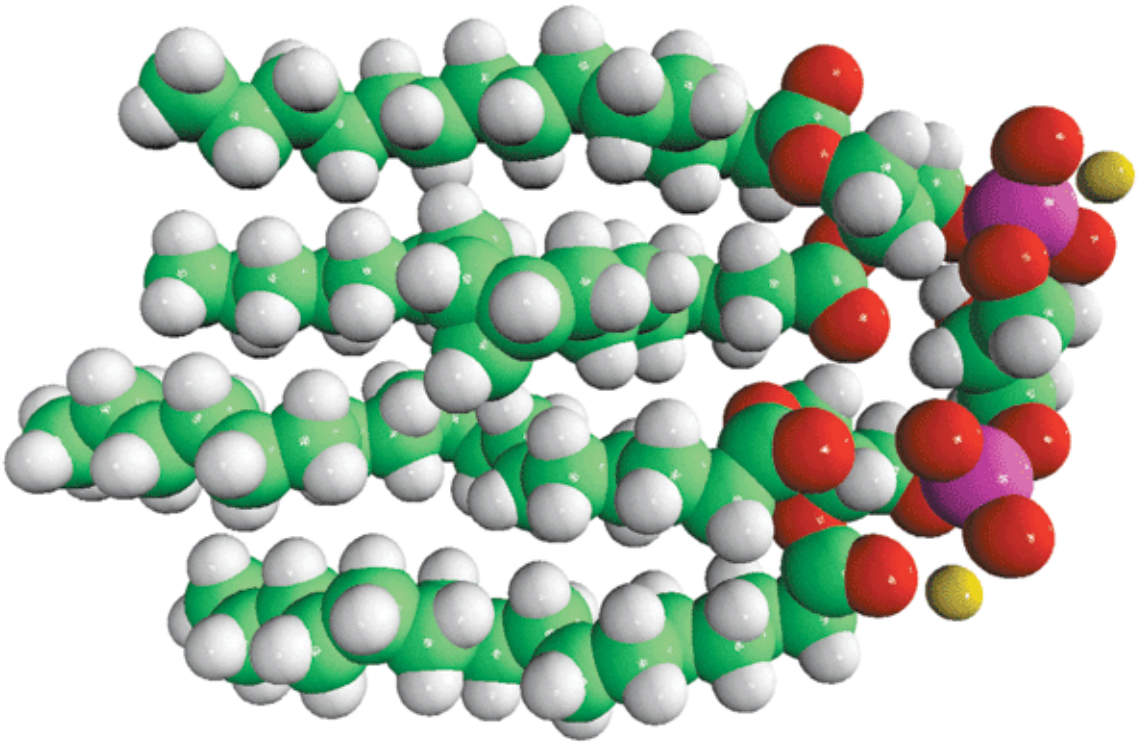

Glycoglycerollipids are another 'specialized' group, found at high percentages in chloroplast membranes, and gram-positive bacteria

There are two major glycolipids

diglyceride ≡ diacylglycerol

monogalactosyldiglyceride (*) (MGDG)
and digalactosyldiglyceride (DGDG)

(*)

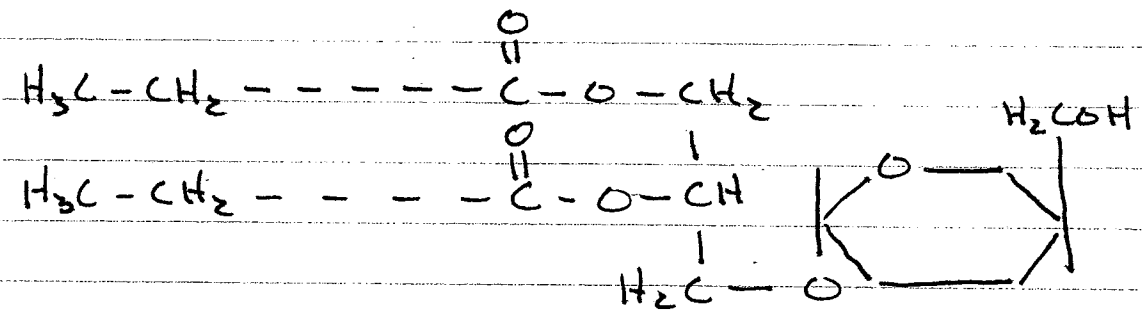

(galactose).

Glycerolipid compositions (% total acyl lipid)

	chloroplast	mitochondria	plasma membrane
MGDG	51	0	0
DGDG	26	0	0
SL[1]	7	0	0
PC	3	27	32
PS	0	25	0
PE	0	29	46
CL[2]	0	20	0
PI	1	0	19
PG[3]	7	0	0

1) sulfolipid
2) cardiolipin
3) phosphatidylglycerol

source: Heldt Pl. Biochem. & Molec. Biol. 1997 page 324.

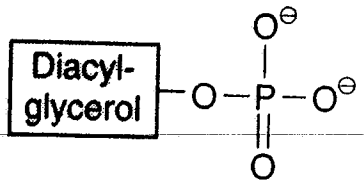

Phosphatidic acid
PA

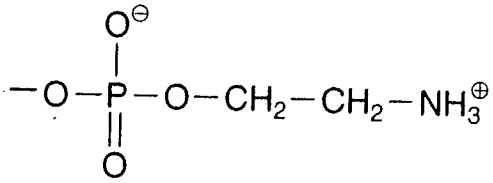

Phosphatidylethanolamine
PE

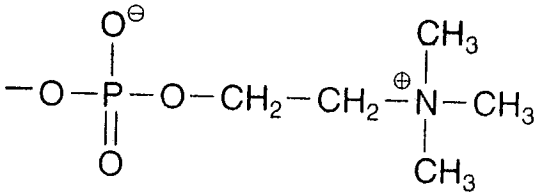

Phosphatidylcholine
(Lecithin) PC

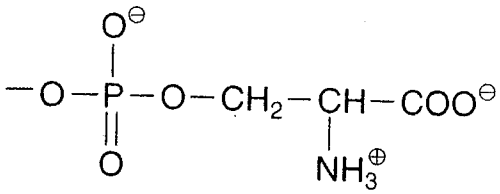

Phosphatidylserine
PS

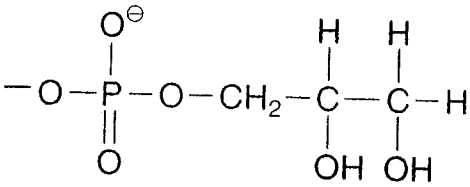

Phosphatidylglycerol
PG

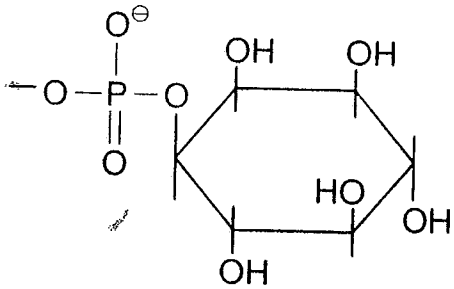

Phosphatidylinositol
PI

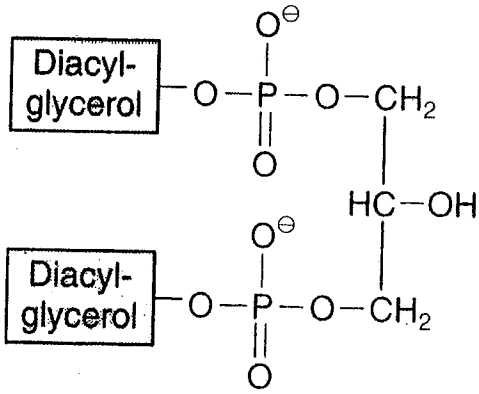

Diphosphatidyl-
glycerol
(Cardiolipin)
CL

Figure 15.5A Hydrophilic constituents of membrane lipids: phosphate and phosphate esters.

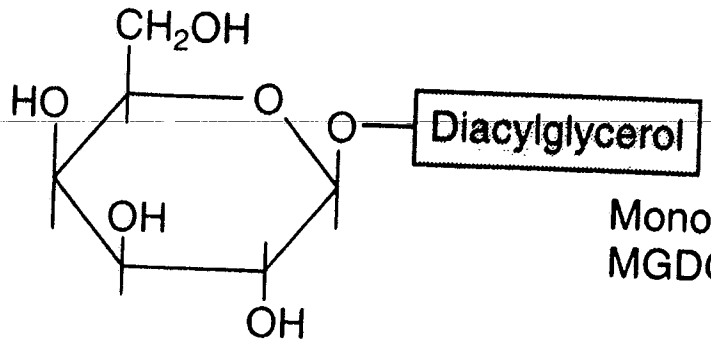

Monogalactosyldiacylglycerol
MGDG

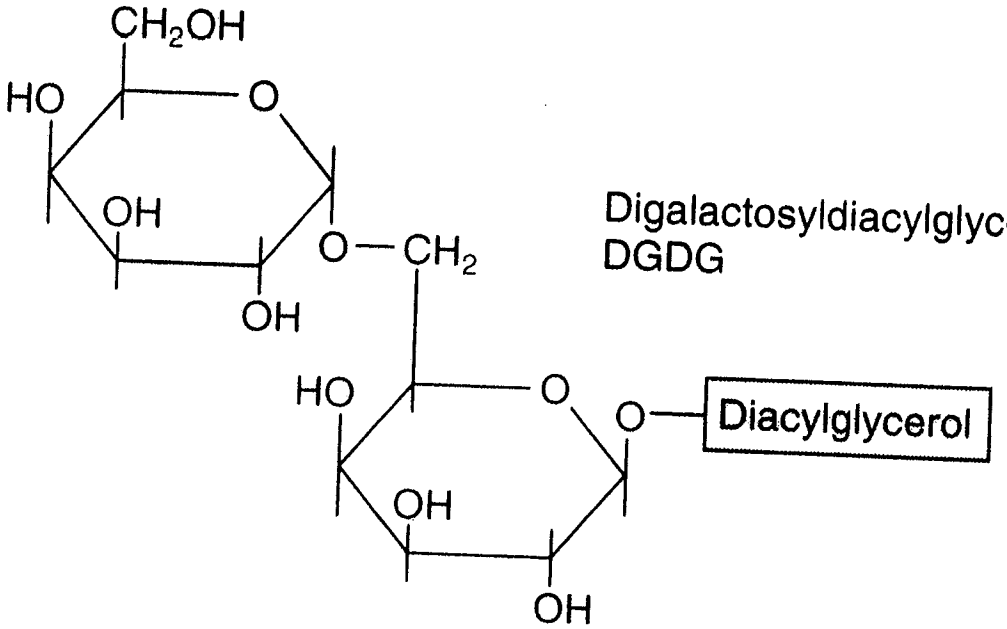

Digalactosyldiacylglycerol
DGDG

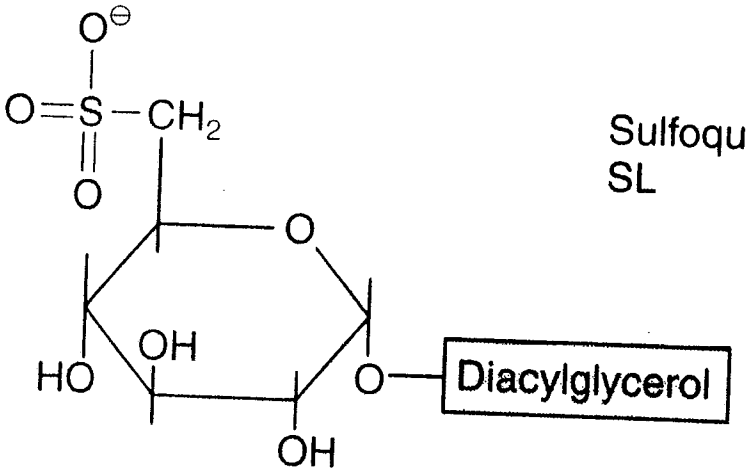

Sulfoquinovosyldiacylglycerol
SL

Figure 15.5B Hydrophilic constituents of membrane lipids: hexoses.

18

Table 15.2 The composition of glycerolipids in various organelle membranes (after Harwood 1980)

Glycerolipids[a]	% of total acyl lipid content		
	Chloroplast thylakoid membrane	Mitochondrial inner membrane	Plasma membrane
MGDG	51	0	0
DGDG	26	0	0
SL	7	0	0
PC	3	27	32
PS	0	25	0
PE	0	29	46
PG	9	0	0
PI	1	0	19
CL	0	20	0

[a] For explanation of abbreviations see Fig. 15.5.

Plant biochemistry and molecular biology

Hans-Walter Heldt
Institute of Plant Biochemistry, Göttingen

with the collaboration of Fiona Heldt

Archaea bipolar lipids.

Although they are well outside the norm, it seems unfair to ignore the third of the three major biological clades (Archaea, the other two clades are Prokaryga and Eukaryga) and its very unusual lipids.

These are bipolar lipids which span completely across the membrane. The membranes formed from these tetraether lipids are very tough, an absolute requirement given that Archaea are generally extremophiles, equally at home in hydrothermal vents and Antarctic ice.

They, or derivatives thereof, have been used in the construction of bioengineered membranes, where stability and impermeability to molecules and ions are the basic specification.

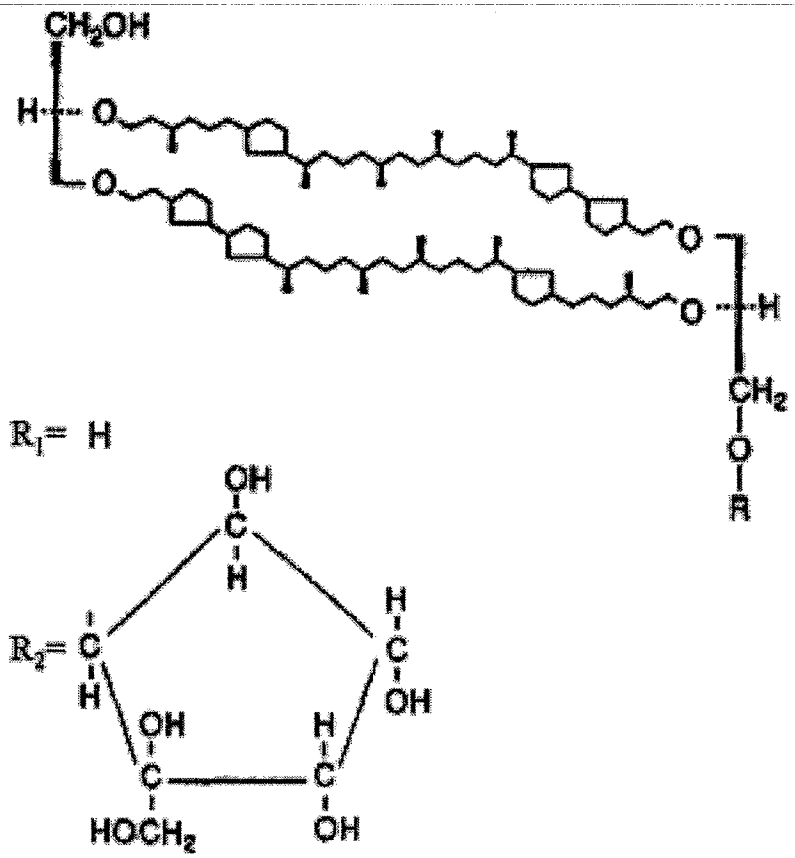

Figure 1. Chemical structure of the hydrophobic backbones that can be obtained by hydrolysis of archaeal tetraether lipids. The number of cyclopentane rings per chain may range from zero to four. R=R1 for GDGT (glycerol-dialkyl-glycerol tetraether), while R=R2 for GDNT (glycerol-dialkyl-calditol-tetraether).

The Archaea Kingdom of microorganisms is believed to be the oldest of the three major clades (Prokarya and Eukarya are the other two clades). Archaea live in extreme environments: from hydrothermal vents under the sea to Antarctic ice fields. Consequently, their membrane composition must be engineered to survive extremes well beyond those normally faced by Prokarya and Eukarya. Their bipolar tetraether lipids span across the membrane (24 to 30 Angstroms wide), with hydrophilic 'heads' at both ends. The membranes formed by the bipolar tetraether lipids are very impermeable to molecules and ions. They are stable over a wide range of temperatures, adaptation to higher temperatures involves additional cyclization of the biphytanyl chains (the cyclopentane rings shown above).

Depending upon preparation method, it is possible to form unilamellar vesicles, highly stable, which may be useful in the development of liposome-mediated drug delivery.

Source: Alessandra Gliozzi, Annalisa Relinia and Parkson Lee-Gau Chong 2002. Structure and permeability properties of biomimetic membranes of bolaform archaeal tetraether lipids. Journal of Membrane Science 206:131-147.

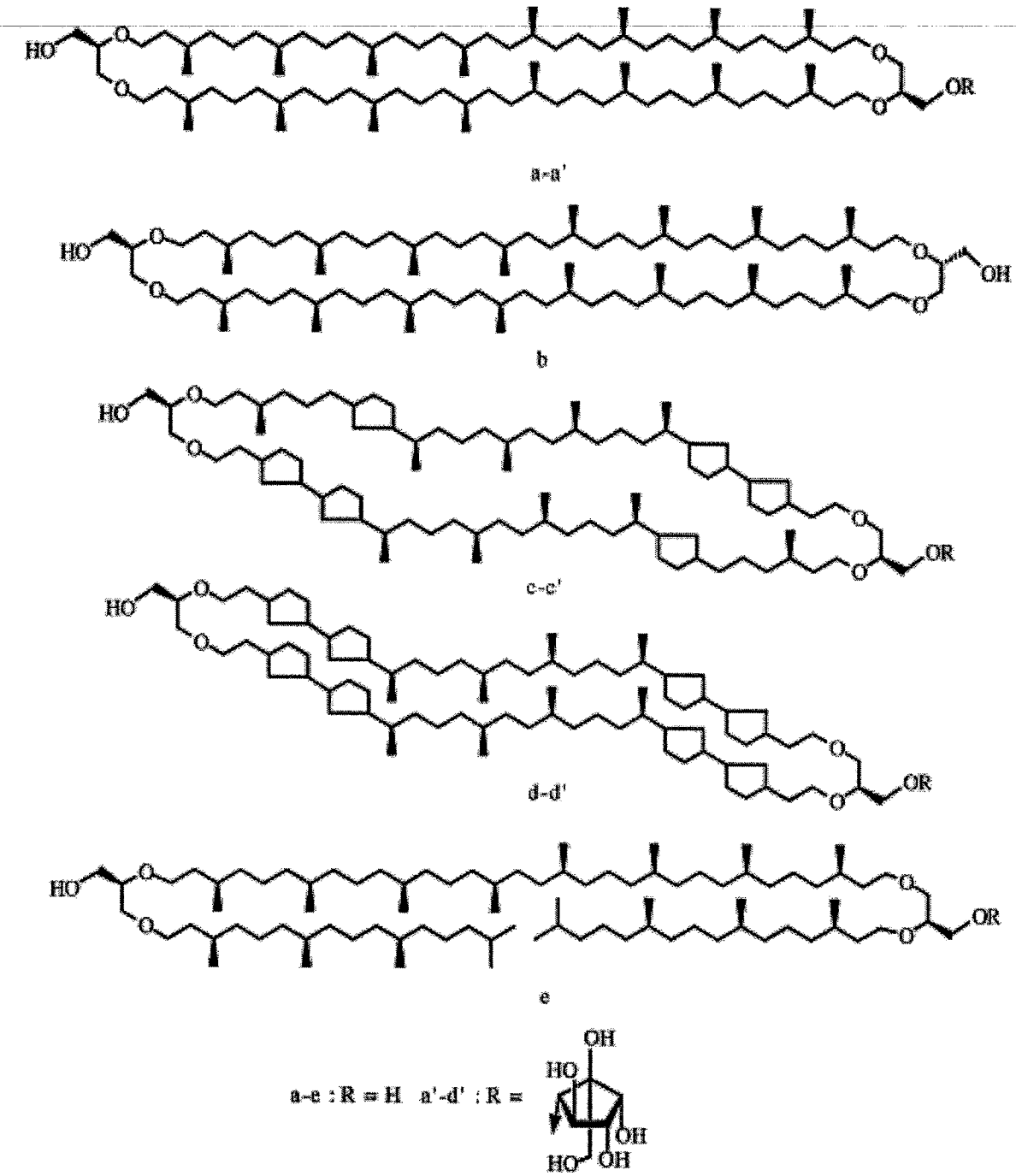

Figure 1. Typical basic structures of caldarchaeol-type (a–e) or calditoglycero-caldarchaeol-type (a′–d′) tetraethers 1 found in methanogenic, thermoacidophilic and some psychrophilic archaeal membrane lipids.

Source: Thierry Benvegnu, Mickaëlle Brard and Daniel Plusquellec 2004. Archaeabacteria bipolar lipid analogues: structure, synthesis and lyotropic properties. Current Opinion in Colloid & Interface Science. 8:469-479

Digression: Lipid Biosynthesis.

The basic process is the addition of 2-carbon units to the growing acyl chain.

The precursor is acetyl-CoA

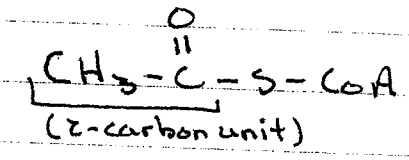

which is formed from either acetate:

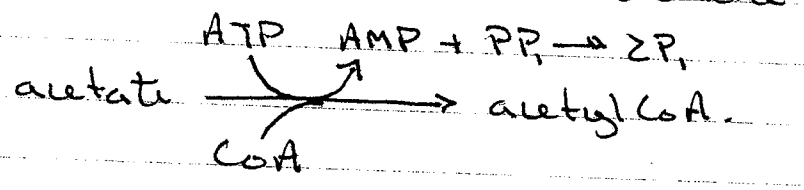

or pyruvate

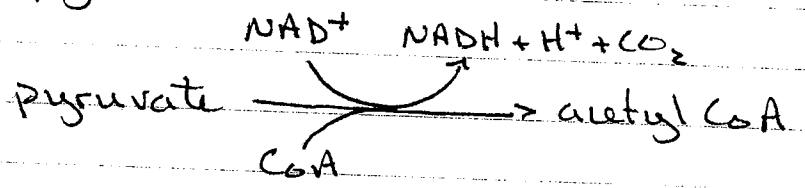

The major energy requirement is reducing equivalents of NADPH + H^+, to reduce the carbonyl (C=O) to CH_2 and ATP in an initial step to produce malonyl CoA.

see overhead.

source: Heldt Pl. Bioch. Molec. Biol. 1997 page 327.

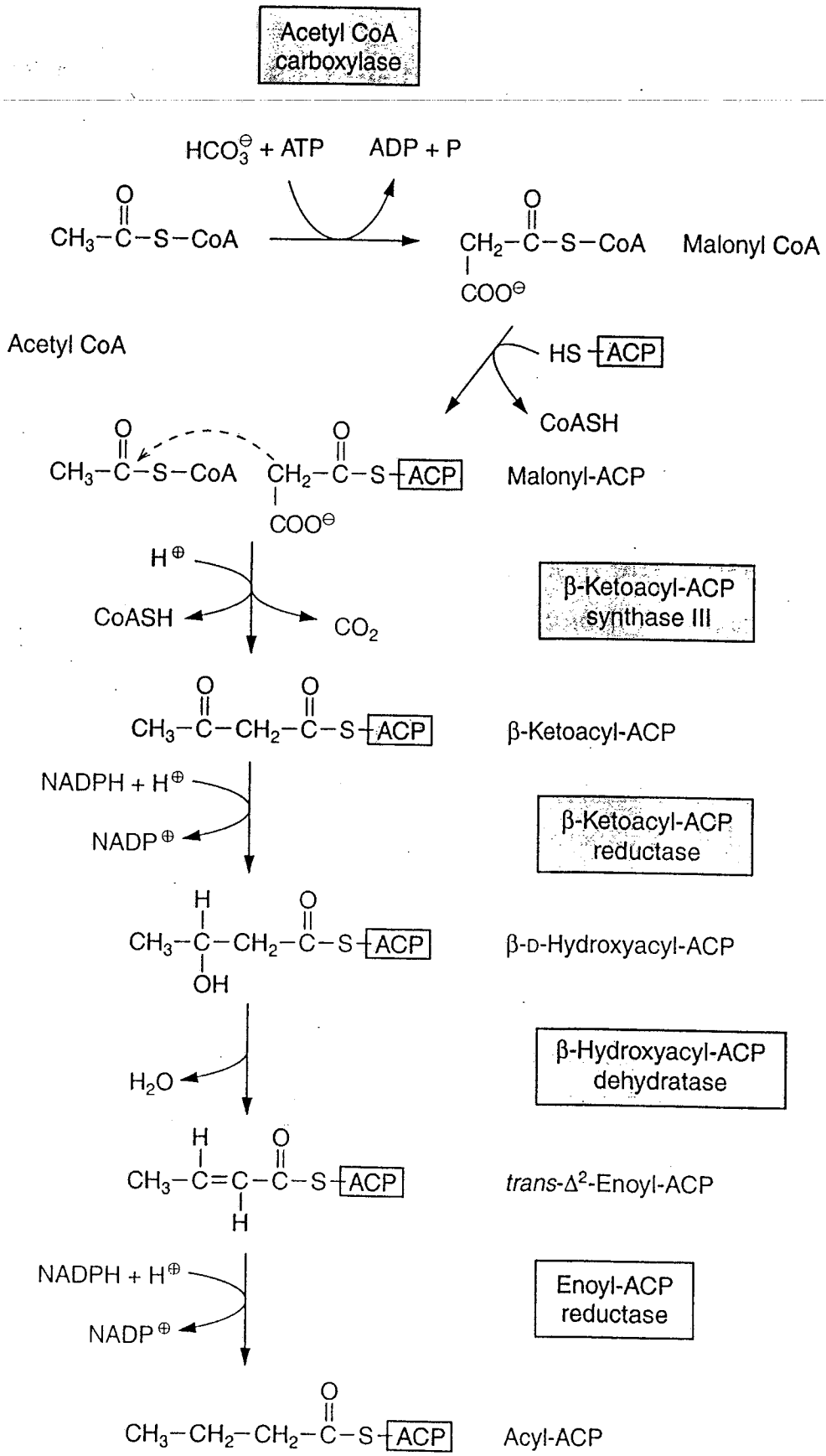

Figure 15.8 Reaction sequence for the synthesis of fatty acids: activation, condensation, reduction, release of water, and further reduction elongate a fatty acid by two carbon atoms.

Acyl chain composition and properties.

The acyl chain is very hydrophobic. The carbon backbone is flexible. With unsaturation (carbon double bonds), backbone flexibility is decreased. The acyl chain flexibility is a primary determinant of membrane fluidity.

In general, flexibility/fluidity varies with

i) the length of the acyl chain: the longer the chainlength, the lower the fluidity.

ii) the presence of unsaturated bonds: unsaturation increases fluidity due to a decrease in 'packability'.

A measure of fluidity is the fact that acyl chains exist in two distinct states (phases):

i) liquid-crystalline (fluid state)

ii) crystalline (gel state)

The transition between the two states occurs at a specific temperature, $T_{m(melt)}$ which is well-defined for specified chain lengths and degrees of unsaturation.

The transition between the two phases is normally measured using differential scanning calorimetry:

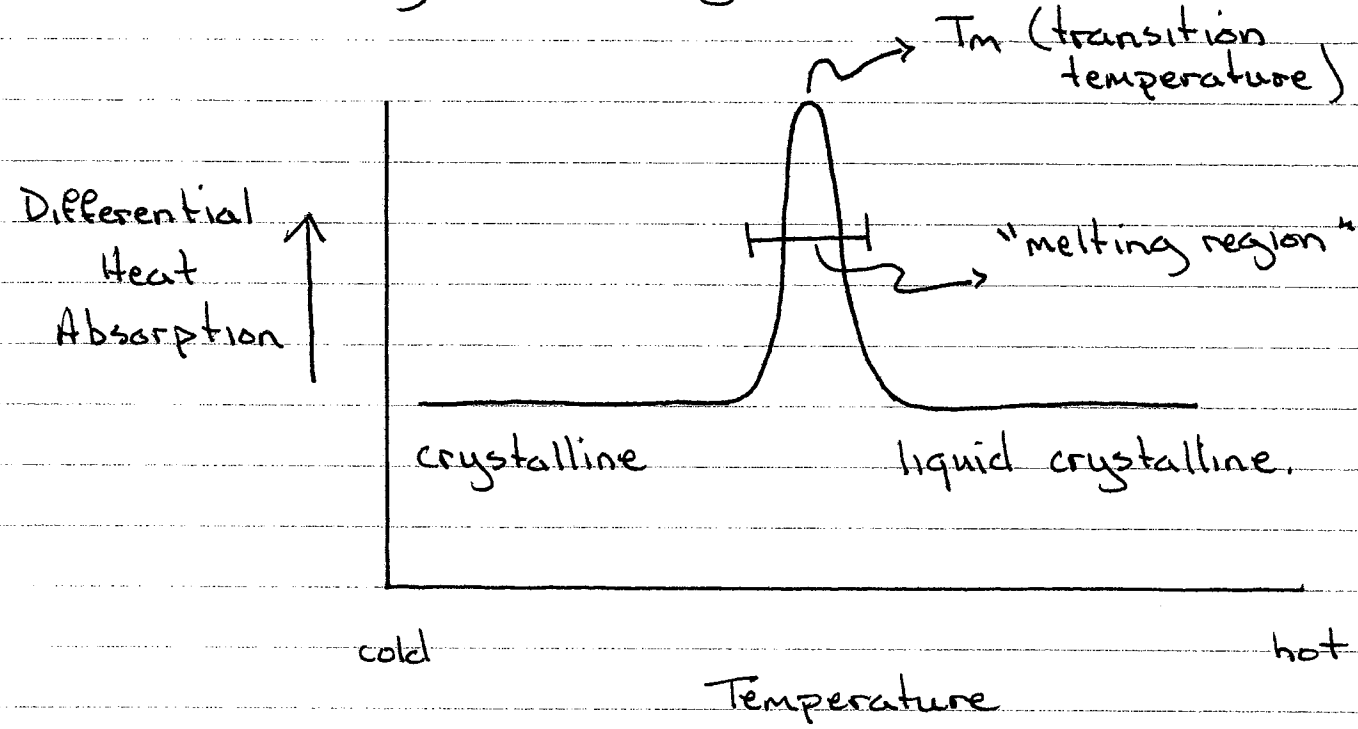

Tm, as a function of chainlength, and headgroup.

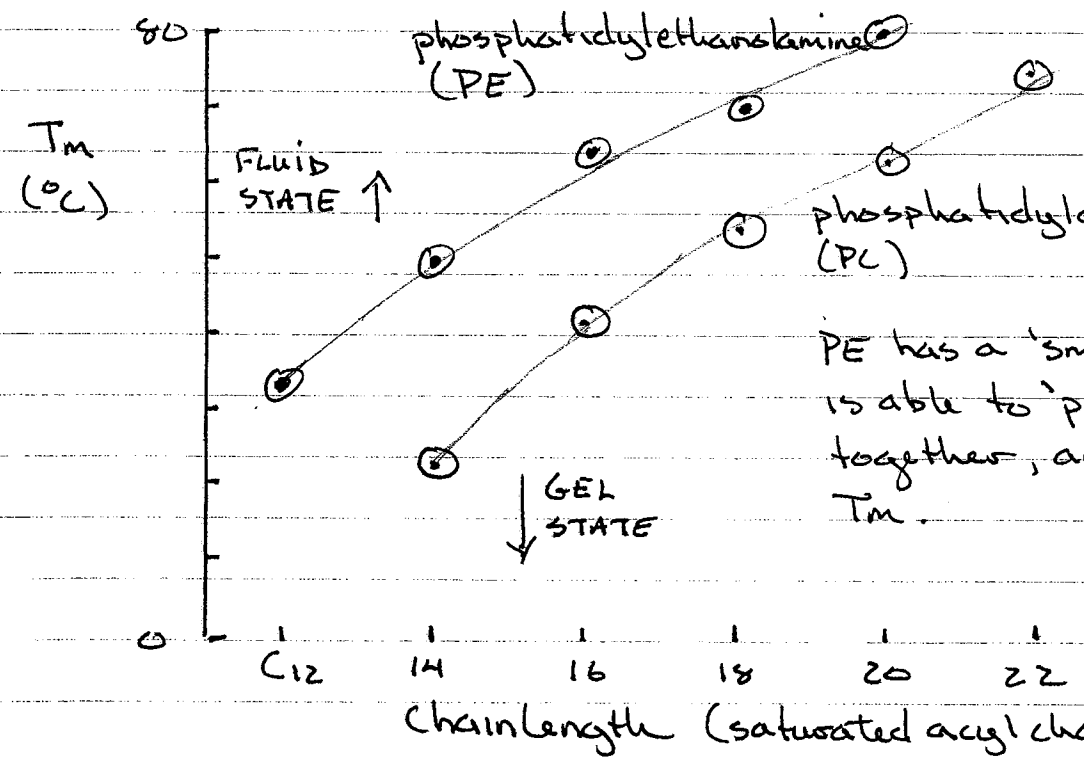

PE has a 'smaller' head-group, is able to 'pack' closer together, and has a higher Tm.

source: Gennis 1989 page 69.

These observations on acyl chain properties are based upon very simplified, well-defined model membranes.
In biological membranes, there are mixtures of acyl chain lengths.

Gennis (1989)* tabulates some data for rat liver.

	14:0	15:0	16:0	16:1	17:0	18:0
mitochondrial (inner)	0.3	27.1	3.6	18.0	16.2	15.8
plasma membrane	0.9	36.9	—	31.2	6.4	12.9

	18:1	18:2	18:3 20 20:1 20:2	20:3	20:4	22:6
mitochondrial	—	—	—	1.0	18.5	3.8
plasma membrane	tr	tr	—	—	11.1	—

* page 27.

So, transitions from fluid to gel are not well-defined. (if present at all)

Although very little is known about membrane protein structure, its dependence on membrane lipid properties has been well characterized.

For example, the ability of the protein to 'fit' in the membrane affects its enzymatic activity

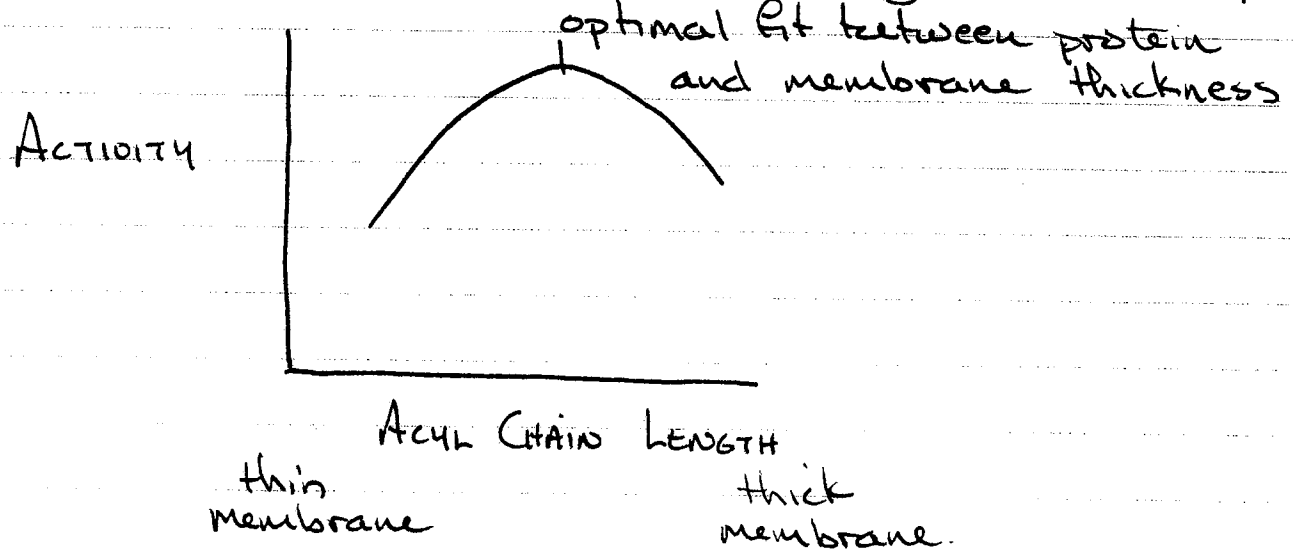

The fluidity of the membrane can also affect enzyme activity

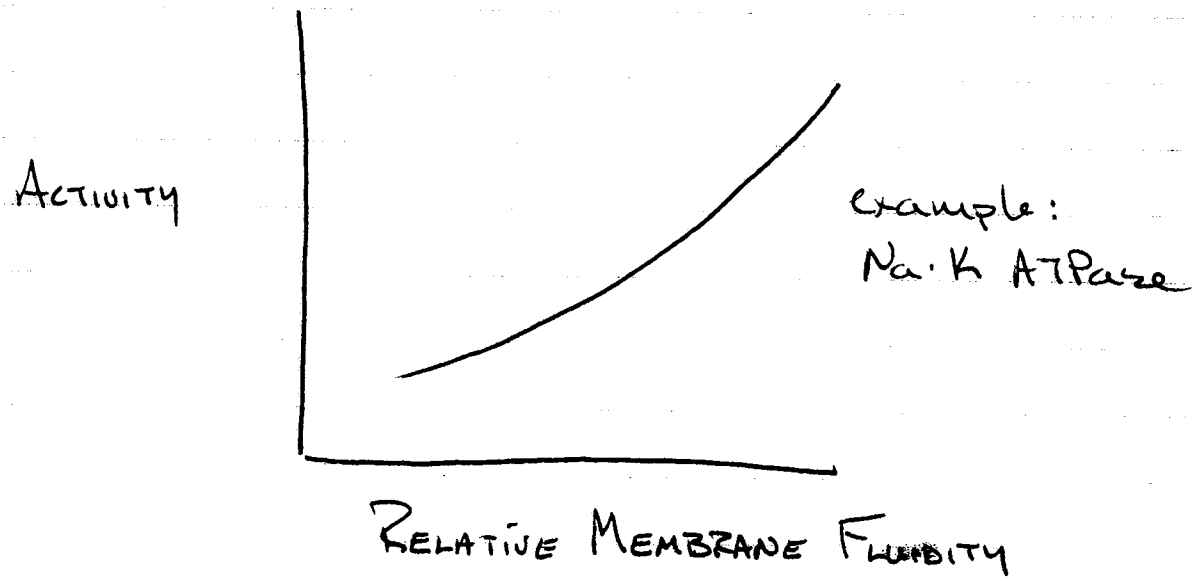

In certain instances, it is clear that membrane fluidity affects the activity of enzymes located in the membrane.

For example the Na^+/K^+ ATPase shows a dependence on membrane fluidity. Normally, fluidity would be modified by changing temperature. However, temperature would have a direct effect on the enzyme. To avoid this, hydrostatic pressure was used to modify fluidity, confirmed using measurements of fluorescence polarization of lipid probes (*). The result was clear: modulating fluidity modulates enzyme activity. PRESENT DATA

(*) see explanation, next page.

There are other instances where the response of an enzyme to membrane properties is more complex.

The glucose transporter from erythrocytes is a well studied example. General conclusions:

The order of importance of bilayer features.

most
1. lipid head group — PS > PA > PG >> PC
2. acyl chain length — $C_{18} > C_{16} > C_{14}$

least
3. 'fluidity'

modified from: Carruthers A & DL Melchior 1986 How bilayer lipids affect membrane protein activity. TIBS 11:331–335.

Because enzyme activity is temperature dependent, it is necessary to modulate the membrane fluidity without changing the temperature. This can be done using hydrostatic pressure to compress the acyl chains.

To measure membrane fluidity, it is common to use a fluorescent reporter probe.

for example, perylene.

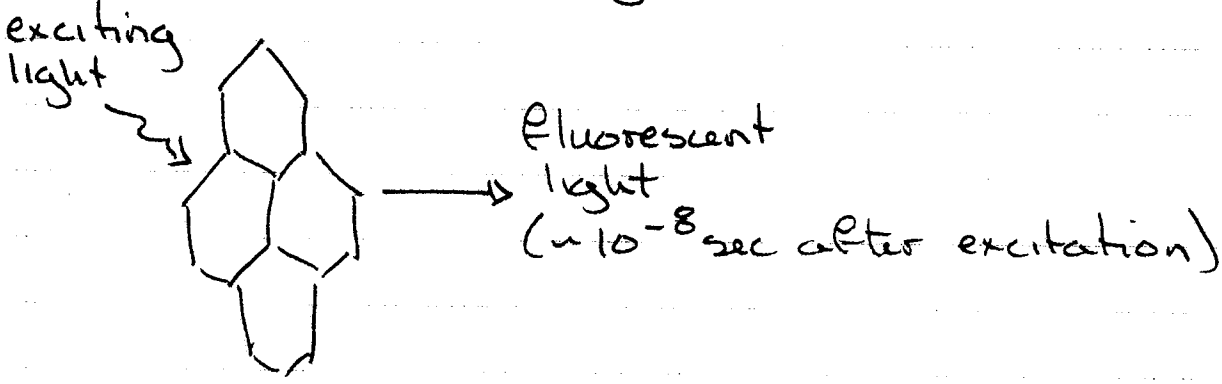

if the exciting light is polarized, the fluorescence will also be polarized UNLESS, the probe changes its orientation within 10^{-8} sec.

$$\text{fluidity} \approx \frac{I_{\parallel} - I_{\perp}}{I_{\parallel} + 2 I_{\perp}}$$

$I_{\parallel}$: flourescence parallel to exciting beam

$I_{\perp}$: fluorescence perpendicular to exciting beam

Experimentally fluorescence anisotropy is the difference between fluorescence intensities emitted parallel to and perpendicular to the polarity of the exciting light, divided by the total emitted fluorescence[1]:

$$A = (I_{\parallel} - I_{\perp}) / (I_{\parallel} + 2 \bullet I_{\perp})$$

where $2 \bullet I_{\perp}$ refers to the two perpendicular directions of emission (perpendicular to the y-axis, as shown below, and perpendicular to the x-axis (parallel to the y-axis).

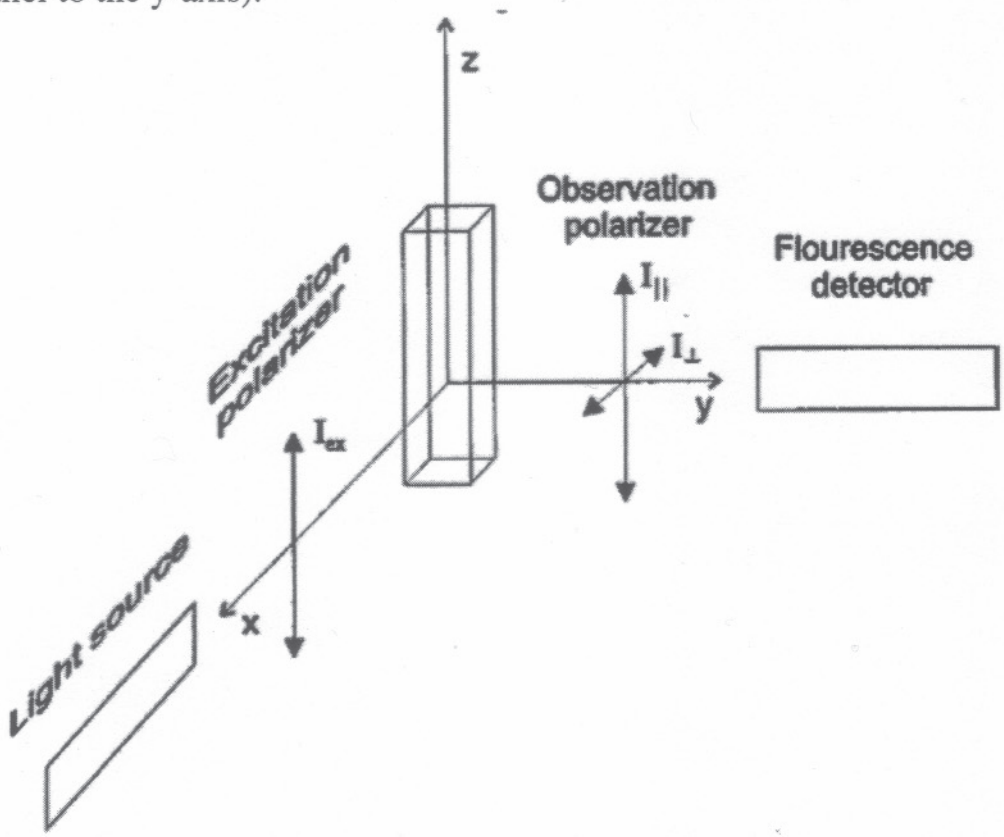

FIG. 1. Schematic diagram for measurement of fluorescence anisotropy of a cylindrically symmetrical emission field.

In the older literature, polarization was commonly used:

$$P = (I_{\parallel} - I_{\perp}) / (I_{\parallel} + I_{\perp}).$$

[1] Source: Bloomfield, VA (2000) Survey of biomolecular hydrodynamics. On-Line Biophysics Textbook Volume: Separations and Hydrodynamics (Todd M. Schuster, editor) Chapter 1

In certain instances, it is clear that membrane fluidity affects the activity of enzymes located in the membrane.

For example the Na^+/K^+ ATPase shows a dependence on membrane fluidity. Normally, fluidity would be modified by changing temperature. However, temperature would have a direct effect on the enzyme. To avoid this, hydrostatic pressure was used to modify fluidity, confirmed using measurements of fluorescence polarization of lipid probes (*). The result was clear: modulating fluidity modulates enzyme activity. PRESENT DATA

(*) see explanation, next page.

There are other instances where the response of an enzyme to membrane properties is more complex.

The glucose transporter from erythrocytes is a well studied example. General conclusions:

The order of importance of bilayer features.

most	1. lipid head group	PS > PA > PG >> PC
	2. acyl chain length	$C_{18} > C_{16} > C_{14}$
least	3. 'fluidity'	

modified from: Carruthers A & DL Melchior 1986 How bilayer lipids affect membrane protein activity. TIBS 11:331-335.

Effect of pressure and temperature on Na^+ K^+ ATPase activity.

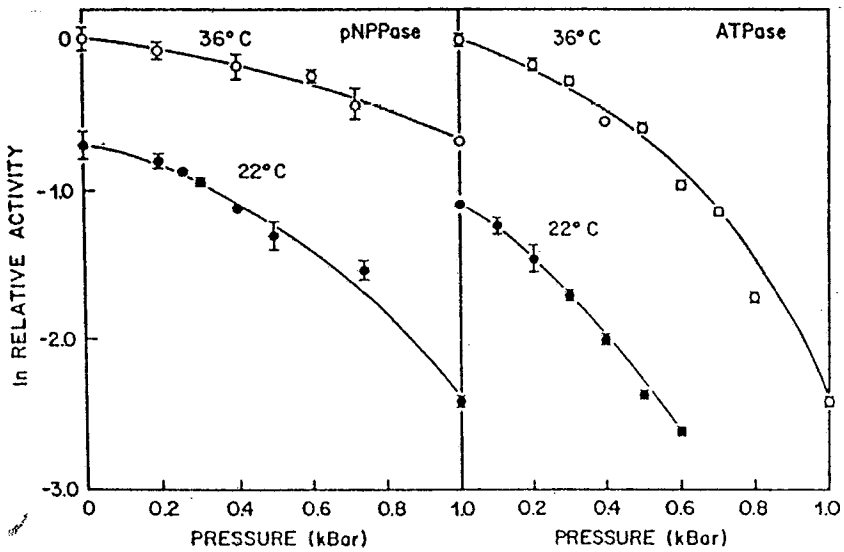

FIG. 2. **Effect of pressure and temperature on (Na,K)-ATPase and K-pNPPase activities.** The rate of ATP or pNPP hydrolysis by the dog kidney (Na,K)-ATPase was measured at the indicated temperature and pressure as described under "Experimental Procedures." The data are plotted as the natural logarithm of the activity normalized to that at 36 °C 1 atm: (Na,K)-ATPase, 13.8 μmol min^{-1} mg^{-1}; K-pNPPase, 2 μmol min^{-1} mg^{-1}.

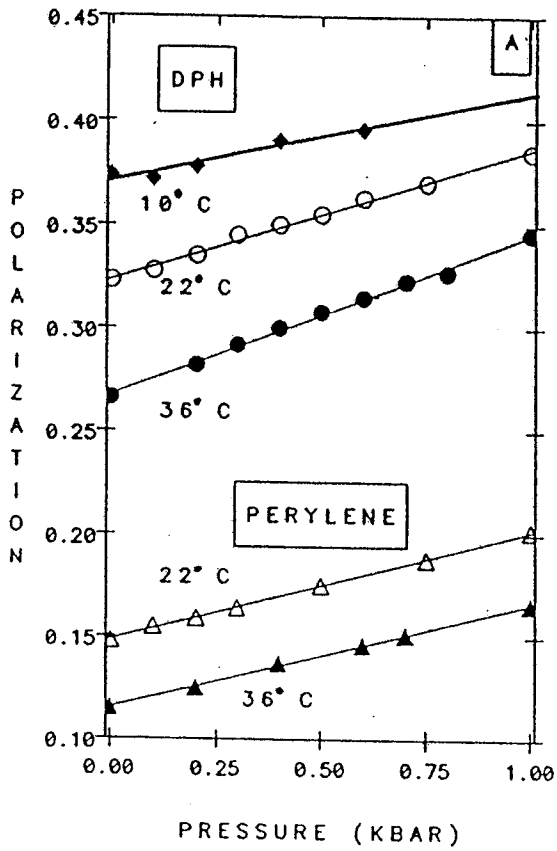

FIG. 3. **Efect of pressure and temperature on the fluorescence polarization of hydrophobic probes in (Na,K)-ATPase.** In *A*, DPH (◆, ○, ●) and perylene (△, ▲) fluorescence polarizations were measured at the indicated temperatures as a function of pressure. Conditions were 50 mM Tris-HCl, pH 7.4, at 22 °C, 100 mM NaCl, 20 mM KCl, 3 mM $MgCl_2$, 2.5 mM EGTA, 3 mM phosphoenolpyruvate, 0.2–0.7 mg/ml dog kidney (Na,K)-ATPase, 4–5 μM DPH or perylene. For DPH, excitation was at 355 nm through a Corning 7-54 filter and emission was measured through 2 mm of a 2 M $NaNO_2$ solution plus a Corning 3-73 filter. For perylene, excitation was at 410 nm, and emission was measured through $NaNO_2$ plus a Corning 3-72 filter.

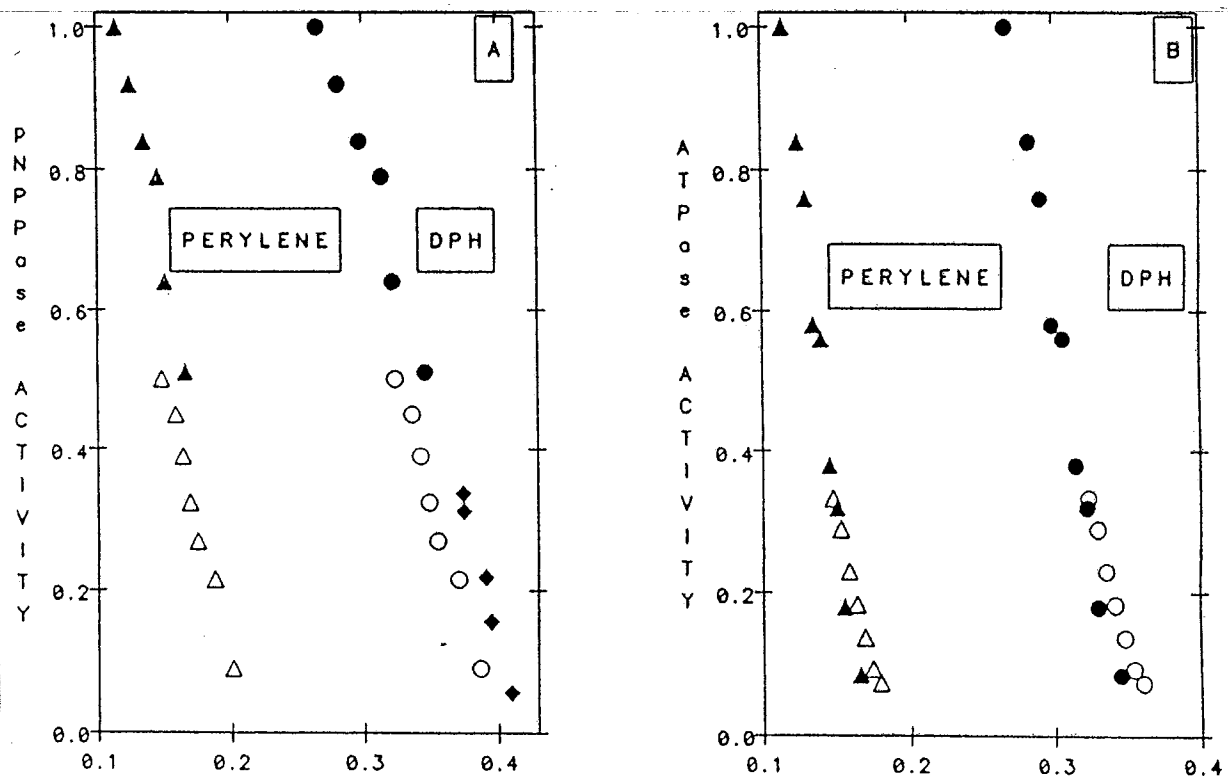

FIG. 5. **Relationship between enzyme activities and fluorescence polarization of lipid probes at different temperatures and pressure.** In *A*, the K-pNPPase activity data, as in Fig. 2, are plotted against the DPH and perylene polarizations (Fig. 3*A*) measured at the same temperature and pressure: ♦, 10 °C; △ and ○, 22 °C; ▲ and ●, 36 °C. In *B*, the (Na,K)-ATPase activity data of Fig. 2 are plotted against the DPH and perylene polarizations (Fig. 3*A*) measured at the same temperature and pressure: △ and ○, 22 °C; ▲ and ●, 36 °C.

So far in this section we have considered energy per *molecule*, whereas in many cases it is more convenient to consider energy per *mole*. To change the Boltzmann distribution from a molecule to a mole basis, we multiply Boltzmann's constant k [energy/(molecule K)] by Avogadro's number N (molecules/mole), which gives us the gas constant R [energy/(mole K)]; i.e., R equals kN.[13] If $n(E)$ and n_{total} are numbers of moles and E is energy per mole, we simply replace k in the Boltzmann energy distribution (Eq. 3.21a) by R:

$$n(E) = n_{\text{total}} e^{-E/RT} \qquad \text{mole basis} \tag{3.21b}$$

For diffusion across a membrane, the appropriate Boltzmann energy distribution indicates that the number of molecules with a kinetic energy of U or greater per mole resulting from velocities in some particular direction is proportional to $\sqrt{T}e^{-U/RT}$ (see Davson and Danielli, 1952). A minimum kinetic energy (U_{min}) is often necessary to diffuse past some barrier or to cause some specific reaction. In such circumstances, any molecule with a kinetic energy of U_{min} or greater has sufficient energy for the particular process. For the Boltzmann energy distribution appropriate to this case, the number of such molecules is proportional to $\sqrt{T}e^{-U_{\text{min}}/RT}$. (These expressions having the factor $\sqrt{T}$ actually only apply to diffusion in one dimension, e.g., for molecules diffusing across a membrane.) At a temperature 10°C higher, the number is proportional to $\sqrt{(T + 10)}e^{-U_{\text{min}}/[R(T+10)]}$. The ratio of these two quantities is called the Q_{10}, or *temperature coefficient* of the process[14]:

$$Q_{10} = \frac{\text{rate of process at } T + 10°\text{C}}{\text{rate of process at } T} = \sqrt{\frac{T + 10}{T}}\, e^{10U_{\text{min}}/[RT(T+10)]} \tag{3.22}$$

13. In this text we will use two analogous sets of expressions: (1) molecule, mass of molecule, photon, electronic charge, k, kT; and (2) mole, molar mass, mole of photons, Faraday's constant, R, RT (see App. I for numerical values of k, R, kT, and RT). As indicated above, a quantity in the second set, which is more appropriate for most of our applications, is Avogadro's number N (6.022×10^{23}) times the corresponding quantity in the first set. We also note that 1 electron volt (eV), an energy unit often used on atomic and molecular levels, equals 1.602×10^{-19} J and that 1 eV molecule^{-1} = 96.55 kJ mol^{-1} = 23.06 kcal mol^{-1} (see App. II).

14. To obtain the form of the exponential given in Equation 3.22, we note that

$$\frac{-U_{\text{min}}}{R(T + 10)} + \frac{U_{\text{min}}}{RT} = \frac{-U_{\text{min}}T + U_{\text{min}}(T + 10)}{RT(T + 10)} = \frac{10U_{\text{min}}}{RT(T + 10)}$$

SOURCE: Nobel PS 1991 Physicochemical and Environmental Plant Physiology. Academic Press. pages 1414.

NOTA BENE: A Q_{10} of 1 is considered passive; a Q_{10} of 2 implies an active (enzymatic) process.

Some enzymes must interact with specific phospholipids for enzymatic activity to be seen.

example β-hydroxybutyrate dehydrogenase (BDH)

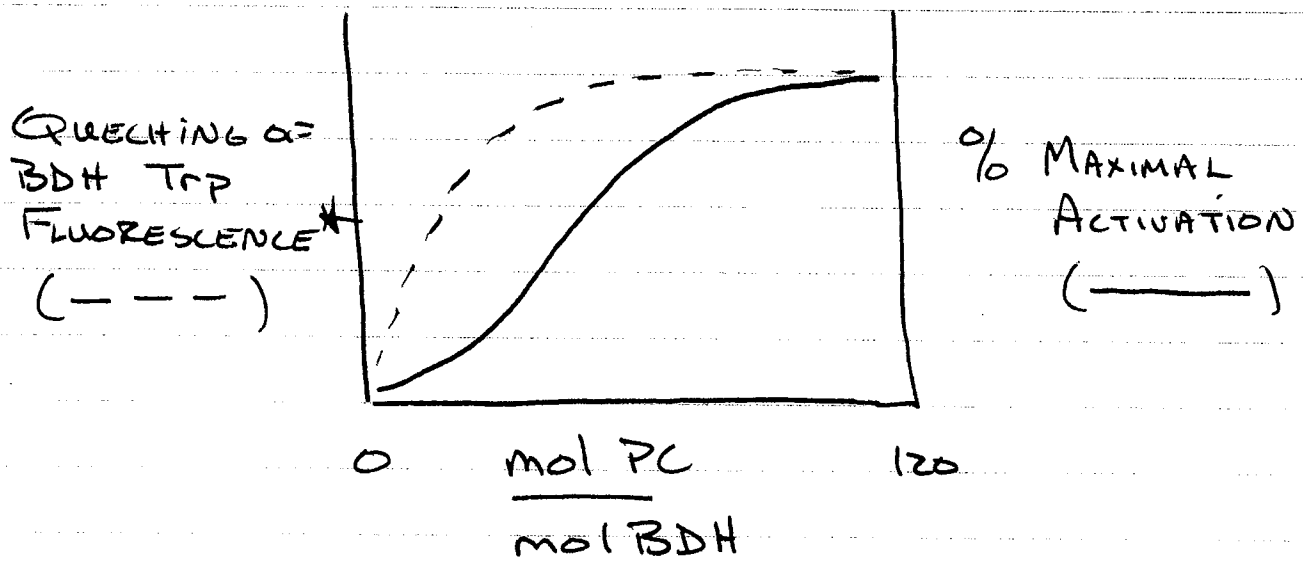

* A fluorescent group on the acyl chain will quench fluorescence of tryptophan amino-acids in the BDH enzyme if the acyl chains are in close proximity to the BDH protein. As quenching increases, more and more acyl chains are interacting with BDH.

Glucose Transporter of Erythrocytes.

<u>nota bene</u> 1:1 stoichiometry of cytochalasin B binding allows the number of transporters <u>to be counted</u>. Very important.

Turnover Number

HEADGROUP

High Tn

Low Tn

PS > PA > PG >> PC

decrease in net charge, surface potential.

ACYL CHAIN

Low Tn

High Tn

$C_{14} < C_{16} < C_{18}$

LIPIDS → sterols

The most common sterol (especially in animals) is cholesterol

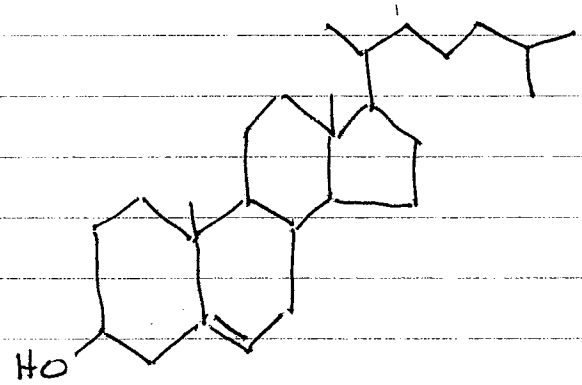

but others, such as sitosterol, stigmasterol, and ergosterol are also common, especially in plants and fungi. The primary differences include unsaturation and addition of C_2H_5 groups.

In animals, cholesterol can be 30% of total lipid by weight, but varies according to cell type. It is found in both the plasma membrane and organellar membranes

Sterols probably have a primary function as packing agents: They cause fluidity to decline and disappearence of the ~~solid~~ gel → liq. transition. (overhead).

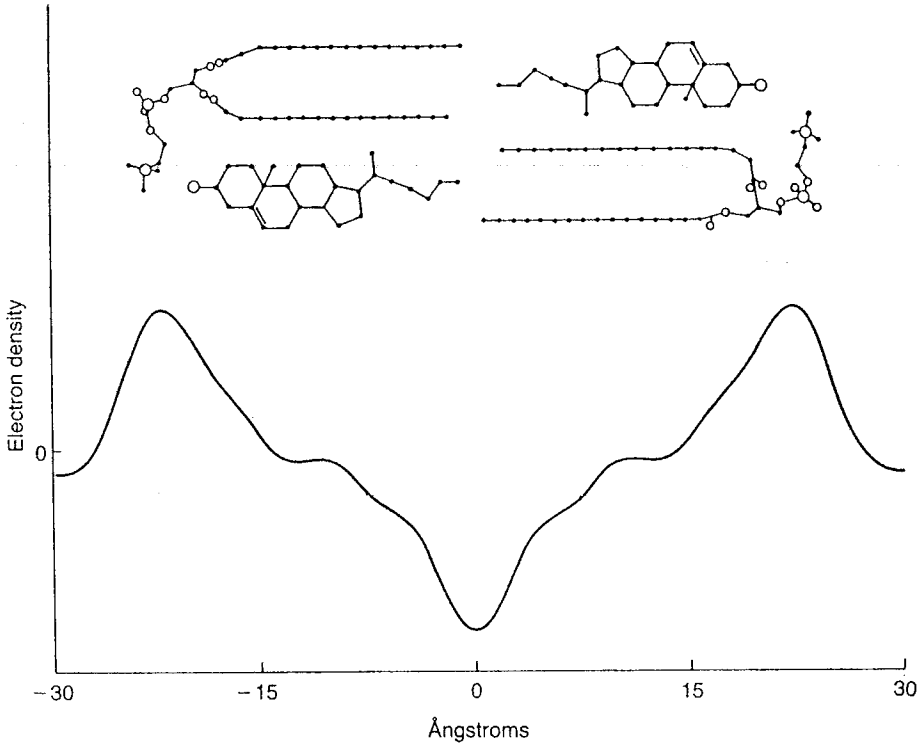

Figure 2.22. Electron density profile of a hydrated bilayer of egg phosphatidylcholine and cholesterol derived from X-ray diffraction analysis. A molecular model consistent with the data is also shown. Adapted from ref. 461.

source Gennis, 1989 page 73

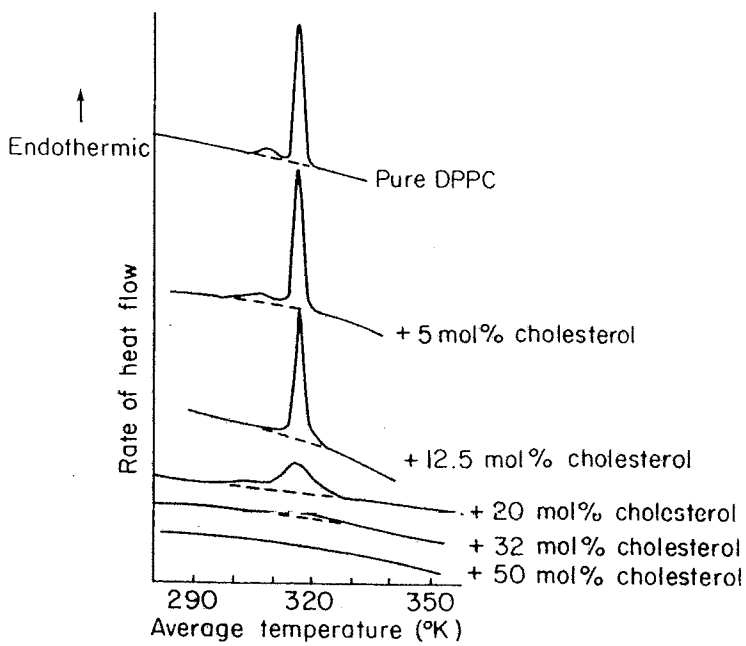

Figure 2.20 Cholesterol abolishes the endothermic lipid phase transition of phospholipids. By increasing the cholesterol content of phospholipid bilayers the endothermic lipid phase transition is gradually moved to lower temperatures, progressively broadened and eventually completely smeared out. Concentrations above 10 mol per cent suffice to abolish the pre-transition of phosphatidyl cholines and concentrations at or above 50 mol per cent completely abolish the endothermic event. These data show the DSC curves for dipalmitoyl phosphatidyl choline–cholesterol mixtures. Similar results can be observed using esr and other physical methods. Increase in temperature, at high cholesterol concentrations, cause a change from a 'relatively ordered' state to a 'relatively disordered' state of the phospholipids. (Reprinted with permission from Ladbroke, B. D., Williams, R. M., and Chapman, D. (1968). *Biochem. Biophys. Acta*, 150, 333–340)

source: Houslay & Stanley 1982 Dynamics of Biological Membranes. page 74.

One aspect of sterol composition of clinical interest is the use of nystatin in treatment of ~~b~~ fungal infections. The susceptibility of pathogenic yeasts to nystatin depends upon the type of sterol (ergosterol makes the yeast susceptible) and the quantity of sterol in the membrane ~~[illegible]~~.

In terms of mechanism, the nystatin molecules penetrate the membrane, interacting with themselves and the ergosterol or some membrane structure created by the ergosterol to form a barrel shaped pore through the membrane.

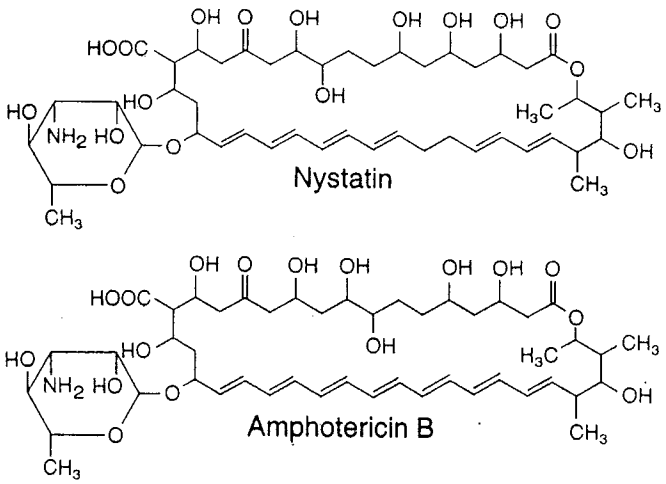

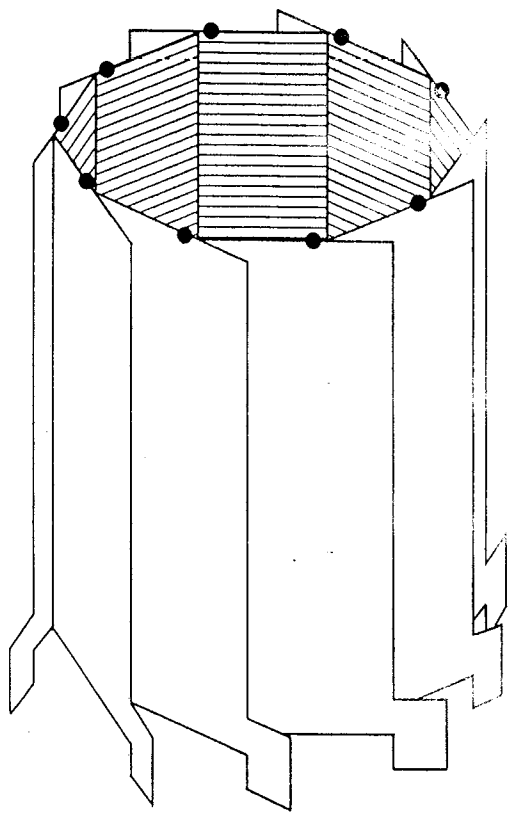

Figure 8.6. Chemical structures of nystatin and amphotericin B, along with a "barrel stave" model of the channel which forms when these polyene antibiotics are in membranes. The protuberance on the bottom represents the amino sugar and the shaded interior represents the hydrophilic polyhydroxyl portion of the molecule. The exterior surface of the channel is completely nonpolar. Adapted from refs. 762 and 959a.

FROM Gennis Biomembranes.

These are antibiotics which kill the cell by forming pores in the membrane, causing uncontrolled loss of cytoplasmic metabolites. Nystation has a clinical use in topical applications to combat yeast infections.

PROTEINS → intrinsic - by definition, proteins which are embedded in the hydrophobic region of the membrane.

<u>reading</u> Cowan SW & JP Rosenbusch 1994 Folding pattern diversity of integral membrane proteins. Science <u>264</u> 914-916.

It is energetically 'difficult' to put a polar/charged molecule into a hydrophobic environment.

For example, the free energy differences for transfer from water into ethanol for amino acids:

		kcal/mol
	leucine (L)	-2.4
	Isoleucine (I)	—
	Valine (V)	-1.7
	Alanine (A)	-0.7
2	Phenylalanine (F)	-2.6
	Methionine (M)	-1.3
	Cysteine (C)	—
3	Threonine (T)	-0.4
	Serine (S)	-0.005
1	Tryptophan (W)	-3.2
	Tyrosine (Y)	-2.4
	Lysine (K)	—
4	Glutamine (Q)	+0.1
	Asparagine (N)	+0.0
	Glutamic Acid (E)	+2.9
	Histidine (H)	-0.45
5	Aspartic Acid (D)	+3.4

nb note that ethanol is polar, due to the hydroxyl. Thus, solvation in hydrocarbon would shift the free energies in a more positive direction.

Table A.2. Two amino acid data bases used to determine hydrophobicity indices of membrane proteins

Side chain	Hydropathy index[a]	Normalized hydrophobicity index[b]
Isoleucine	4.5	1.4
Valine	4.2	1.1
Leucine	3.8	1.1
Phenylalanine	2.8	1.2
Cysteine/cystine	2.5	0.29
Methionine	1.9	0.64
Alanine	1.8	0.62
Glycine	−0.4	0.48
Threonine	−0.7	−0.05
Tryptophan	−0.9	0.81
Serine	−0.8	−0.18
Tyrosine	−1.3	0.26
Proline	−1.6	0.12
Histidine	−3.2	−0.40
Glutamic acid	−3.5	−0.74
Glutamine	−3.5	−0.85
Aspartic acid	−3.5	−0.90
Asparagine	−3.5	−0.78
Lysine	−3.9	−1.5
Arginine	−4.5	−2.5

[a] From Kyte and Doolittle (1982).
[b] From Eisenberg (1984).

Initial predictive models focussed on side chain properties (Kyte & Doolittle 1982. J. Molec. Biol. 157: 105-132); the major refinement is been to quantify the free energy difference for transfer of an α-helix from an aqueous solution into a membrane domain (Goldman, Engelmann & Steitz 1986. Ann. Rev. Biophys. ~~Bio~~Biophys. Chem. 15 321-353).

An additional membrane-traversing structure is β-pleated sheet where carbonyl's and imino's hydrogen-bond between two adjacent strands of the peptide. In this case, a shorter sequence of amino acids would be required to traverse the membrane.

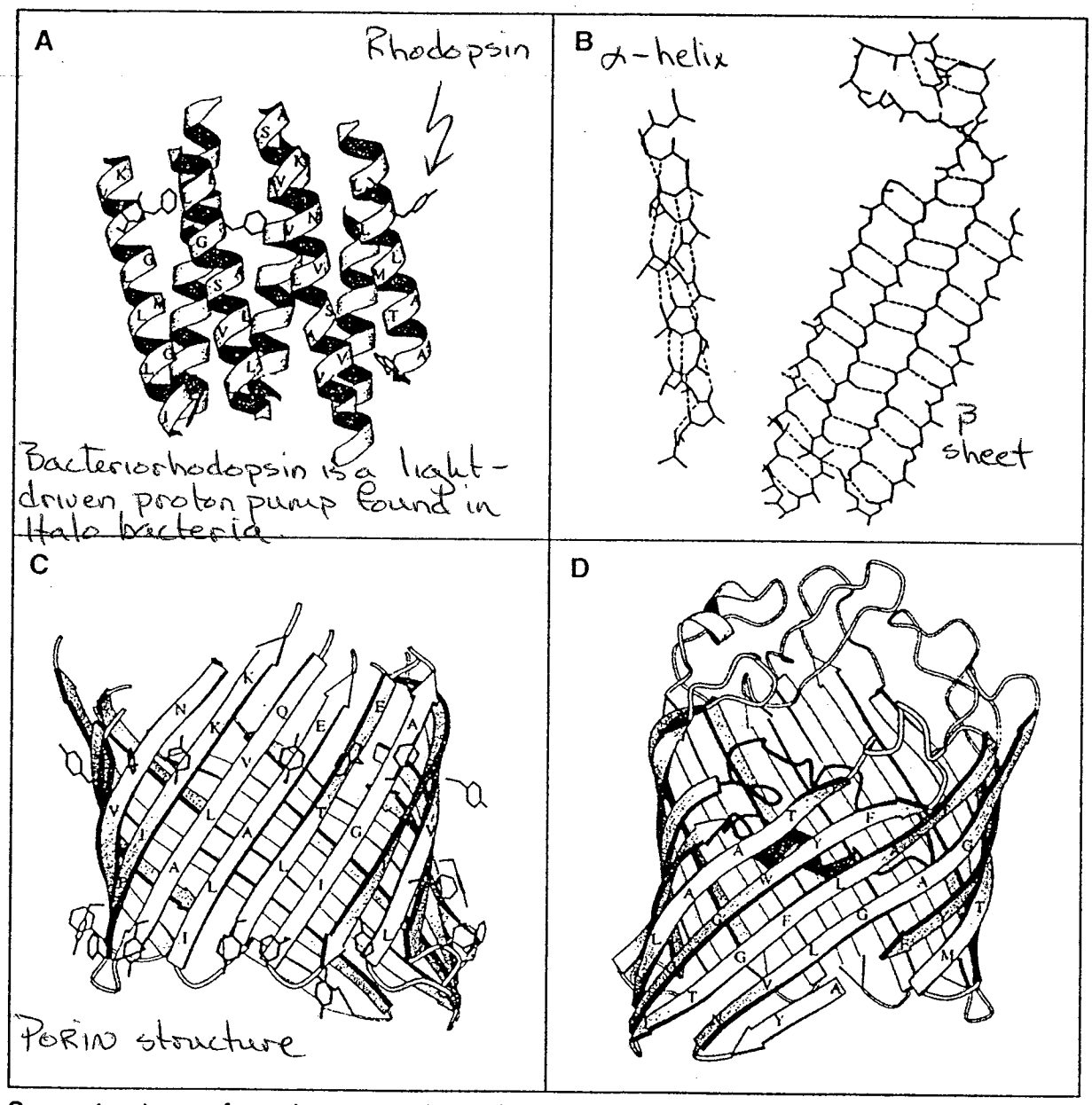

Some structures of membrane proteins. (A) Bacteriorhodopsin, an α-helical transmembrane protein. Its seven α helices are viewed from within the plane of the membrane and shown without connecting loops. Residues facing the viewer are labeled in the single-letter code, with aromatic groups shown in full. **(B)** Saturation of the hydrogen-bonding potential in peptides within membrane boundaries. At left is an α helix from bacteriorhodopsin. The hydrogen-bonding potential is saturated by *intra*segmental bonds (dotted lines). On the right, four β strands from porin show how all hydrogen bonds are saturated *inter*segmentally. **(C** and **D)** Two views of the porin monomer. Each monomer is a highly regular β barrel with 16 antiparallel β strands. Panel C highlights the segregation of nonpolar and polar residues. Individual strands are connected to their nearest neighbors by short turns on the periplasmic side (bottom) and by longer loops (truncated here for clarity) on the extracellular face of the protein (top). The surface exposed to lipids consists of short, aliphatic residues. Panel D shows the opposite face of the barrel where residues are involved in interactions with neighboring subunits (near the threefold molecular axis). In this representation, the external loops forming the channel entrance are shown. One loop (in red) folds into the channel and forms the constriction. It lies within the membrane boundaries but is not in contact with lipids. Diagrams were produced with the programs "Molscript" and "O" (*23*).

But note that it is not only the side chains of the amino acids which affect solvation in an oil, but also the carbonyl ($\dot{C}=O$) and imino ($\dot{N}-H$) groups of the peptide bond

which should not be available for interaction with the hydrophobic hydrocarbon ($-\overset{H}{\underset{H}{C}}-$) groups of the acyl chains.

To solve this problem, the simplest model is an alpha-helix (carbonyl's hydrogen bonded to imino's) with hydrophobic side chains.

With this configuration, it would take approximately 15-25 amino acids to traverse the hydrophobic region of the membrane.

The hydrophobic nature of the side chains is predicted by their relative polarity (the hydration potential) and the extent to which such side chains are normally found 'buried' in hydrophobic domains in the well-characterized globular water-soluble proteins.

Kyte and Doolittle pioneered predictive models based upon 'hydropathy' indices (a measure of hydrophobicity which were then refined by others.

(next page)

Table A.1.3 Physical Characteristics of the Amino Acids

Amino acid	3-letter code	1-letter code	Mol. wt. (g/mol)	Accessible surface area[a]	Hydro-phobicity[b]	Relative mutability[c]	Surface probability[d]
Alanine	Ala	A	89.1	115	–0.40	100	62
Arginine	Arg	R	174.2	225	–0.59	65	99
Asparagine	Asn	N	132.1	160	–0.92	134	88
Aspartate	Asp	D	133.1	150	–1.31	106	85
Cysteine	Cys	C	121.2	135	0.17	20	55
Glutamate	Glu	E	147.1	190	–1.22	102	82
Glutamine	Gln	Q	146.2	180	–0.91	93	93
Glycine	Gly	G	75.1	75	–0.67	49	64
Histidine	His	H	155.2	195	–0.64	66	83
Isoleucine	Ile	I	131.2	175	1.25	96	40
Leucine	Leu	L	131.2	170	1.22	40	55
Lysine	Lys	K	146.2	200	–0.67	56	97
Methionine	Met	M	149.2	185	1.02	94	60
Phenylalanine	Phe	F	165.2	210	1.92	41	50
Proline	Pro	P	115.1	145	–0.49	56	82
Serine	Ser	S	105.1	115	–0.55	120	78
Threonine	Thr	T	119.1	140	–0.28	97	77
Tryptophan	Trp	W	204.2	255	0.50	18	73
Tyrosine	Tyr	Y	181.2	230	1.67	41	85
Valine	Val	V	117.1	155	0.91	74	46

[a] Accessible surface area is in $Å^2$ and is for the amino acid as part of a polypeptide backbone (Chothia, 1976).

[b] Hydrophobicity is in arbitrary units and is based on the OMH scale of Sweet and Eisenberg (1983), which emphasizes the ability of amino acids to replace one another during the course of evolution.

[c] Relative mutability is also in arbitrary units (with alanine set to 100) and represents the probability that an amino acid will mutate within a given time. Thus, as two closely related proteins diverge, a given tryptophan residue is only 18% as likely as a given alanine residue to mutate (Dayhoff et al., 1978).

[d] Surface probability is the likelihood that 5% or more of the surface area of an amino acid will be exposed to the solution surrounding a protein (Chothia, 1976). Thus, while some portion of almost all the arginines will help make up the surface of a protein, less than half of the valines will be exposed to solution. To understand in more detail how amino acids are buried, see Rose et al. (1985; for example, although tyrosine is often found exposed to the surface of a protein, a substantial proportion of its surface area is typically buried).

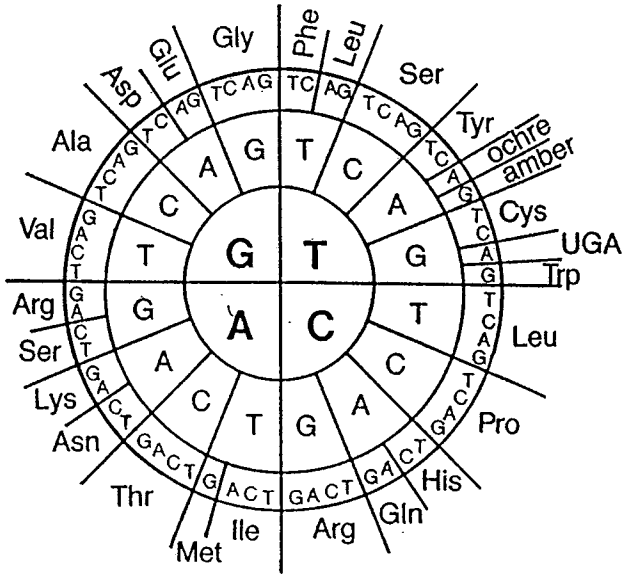

Figure A.1.2 The genetic code. Names of amino acids and chain termination codons are on the periphery of the circle. The first base of the codon is identified in the center ring; the second base of the codon is in the middle ring; and the third base(s) of the codon is in the outer ring of the circle.

page 708

Table 1 Ion pumps classified according to energy source

Energy source	Pump	Transported ion	Occurrence	References
Light	Bacteriorhodopsin	H^+	Halobacteria	1
Light	Halorhodopsin	Cl^-	Halobacteria	2
Redox energy	Cytochrome oxidase	H^+	Mitochondria, bacteria	3
Redox energy	NADH oxidase	Na^+	Alkalophilic bacteria	4
Decarboxylation	Ion-translocating decarboxylases	Na^+	Bacteria	5
Hydrolysis of pyrophosphate	H^+-PPase	H^+	Plant vacuoles	6
ATP hydrolysis	Transport ATPases	H^+, Na^+, K^+, Ca^{2+}	Widely distributed	7

[1]Stoeckenius and Bogomolni (1982), Khorana (1988).
[2]Lanyi (1986), Oesterhelt and Tittor (1989), Lanyi (1990).
[3]Wikström et al. (1985), Gelles et al. (1986), Krab and Wikström (1987).
[4]Tokuda and Unemoto (1984).
[5]Dimroth (1987, 1990).
[6]Rea and Sanders (1987), Hedrich et al. (1989).
[7]Pedersen and Carafoli (1987a,b).

Table 2 Ion-motive ATPases

Subclass	Subunit structure	Transported ion	Phosphorylated intermediate	Inhibitors[a]	Occurrence	References
F-type (F_oF_1)	complex[b]	H^+	No	DCCD, N_3^-	Bacteria, mitochondria, chloroplasts	1
V-type (vacuolar)	Complex	H^+	No	N_3^-, NEM	Cellular organelles	2
P-type (E_1E_2)	α, $\alpha\beta$, $\alpha_2\beta_2$	H^+, Na^+, K^+, Ca^{2+}	Yes	Vanadate	Widely distributed	3

[1]Junge (1982), Schneider and Altendorf (1987), Senior (1988).
[2]Sze (1985), Al-Awqati (1986), Rudnick (1986), Bowman and Bowman (1986), Schneider, (1987), Forgac (1989).
[3]Slayman (1987), Jørgensen and Andersen (1988), Serrano (1989).
[a]Abbreviations: DCCD, dicyclohexylcarbodiimide; NEM, *N*-ethylmaleimide.
[b]For example, $\alpha_3\beta_3\gamma\delta\epsilon ab_2c_{10}$.

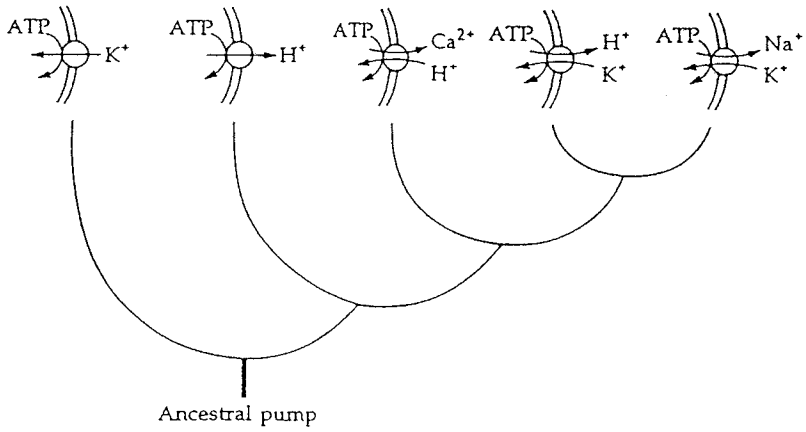

3 Evolutionary tree for the family of cation-pumping ATPases with phosphorylated intermediate (P-type ATPases). (After Serrano, 1988.)

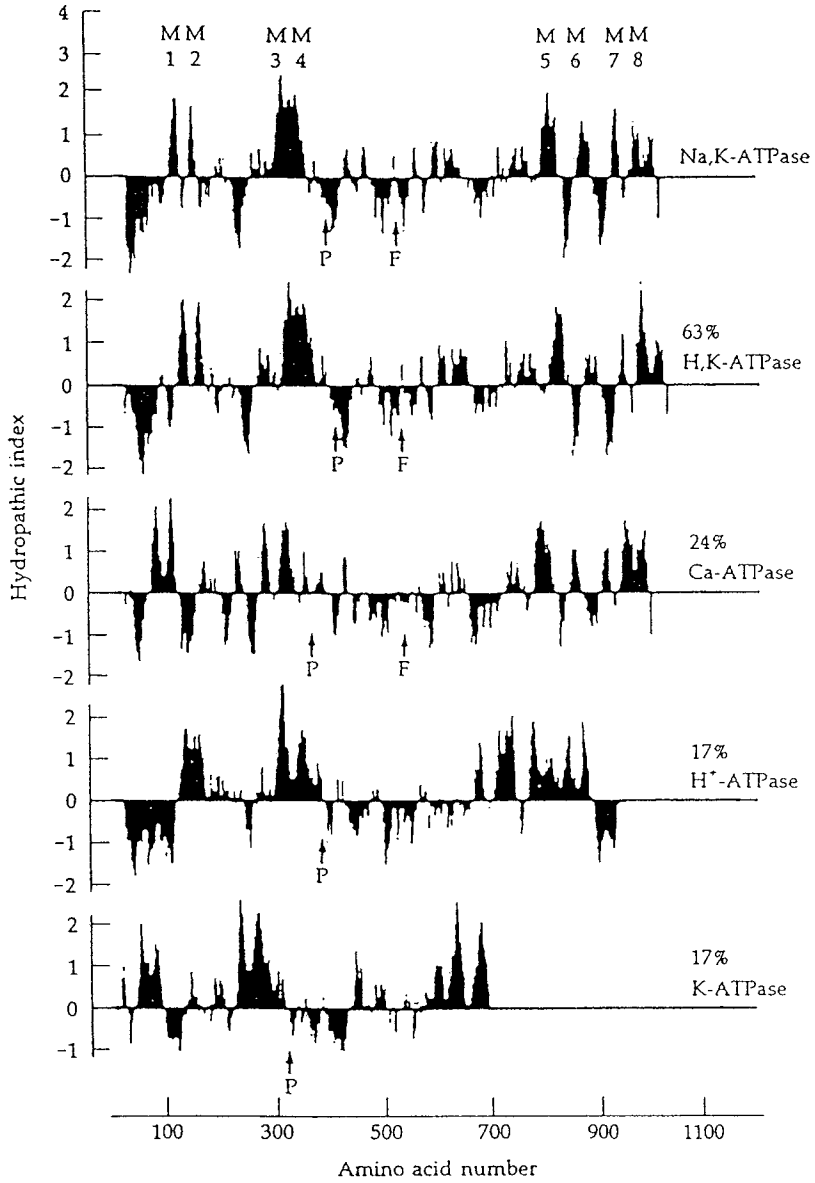

2 Hydropathy plots for P-type ATPases. Positive values of the hydropathic index correspond to apolar stretches in the sequence, negative values to polar stretches. M1–M8 indicate positions of putative transmembrane helices. P is the phosphorylation site and F the ATP-binding site. (From Jørgensen and Andersen, 1988, with kind permission.)

Determination of membrane structure relies upon two techniques.

a) x-ray crystallography
b) electron microscopy and image reconstruction.

X-ray crystallography requires that the protein be crystallized, so that it is sufficiently ordered to deflect x-rays in a well-defined pattern.

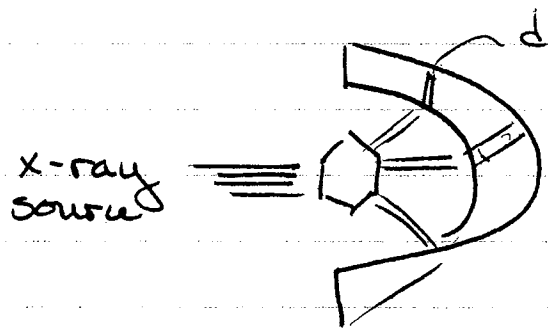

scattering of the x-rays by atoms in the crystal yield a distinct diffraction pattern on x-ray sensitive detector.

To 'solve' the protein structure, one must back-track from the diffraction pattern to the original structure required to cause that particular diffraction pattern.

Example of x-ray crystallography.

reading (not required): Deisenhofer, J & H. Michel 1989 The photosynthetic reaction center from the purple bacterium Rhodopseudomonas viridis. Science 245 1463-1473.

background A photosynthetic reaction center absorbs light, resulting in excitation of an electron to a higher energy state. When excited the electron is donated to an acceptor (quinone) molecule and can be used in the re-dox reactions of photosynthesis. Although it is bacterial in origin, it shows high homology to Photosystem II of higher plants

The key to solving the structure was creation of suitable crystals.

There are three major structural aspects:

1) α-helix, transmembrane segments hydrophobic in nature dominate the structure.
2) the distribution of charged amino acids is assymetric

(next page)

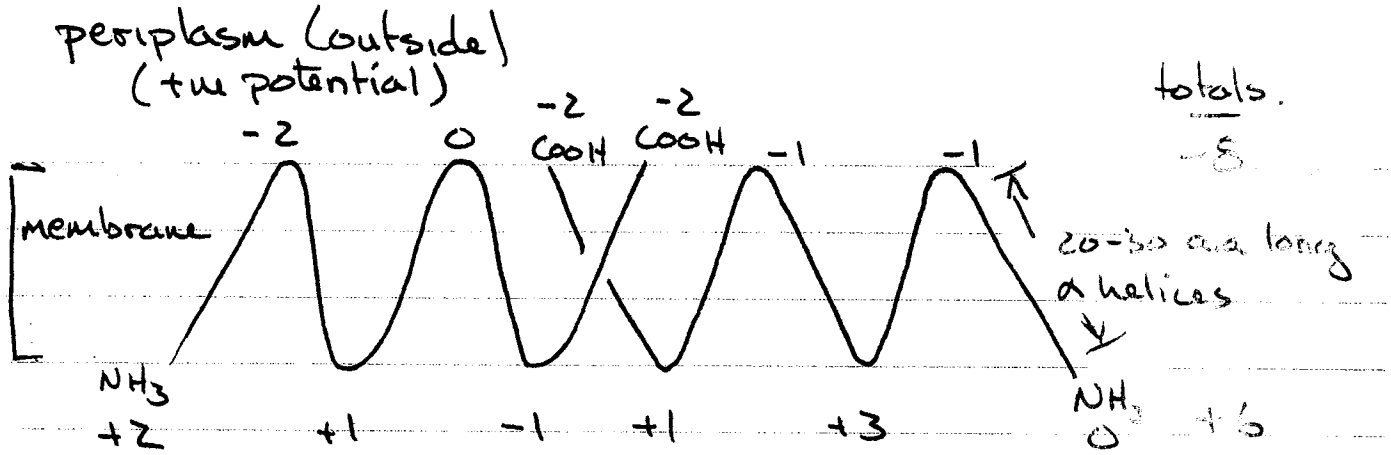

cytoplasm (inside)
(-ve potential)

3) charged structures were isolated in hydrophobic regions - unexpected because it is energetically highly unfavourable.

General: A photosynthetic reaction center, in which an excited electron is transferred across the membrane via the porphyrin molecules

Features: One. alpha-helical transmembrane segments, hydrophobic in nature dominate the structure. Two. The distribution of charged amino acids is assymetric. Three. Charged structures are isolated in hydrophobic regions - energetically highly unfavourable.

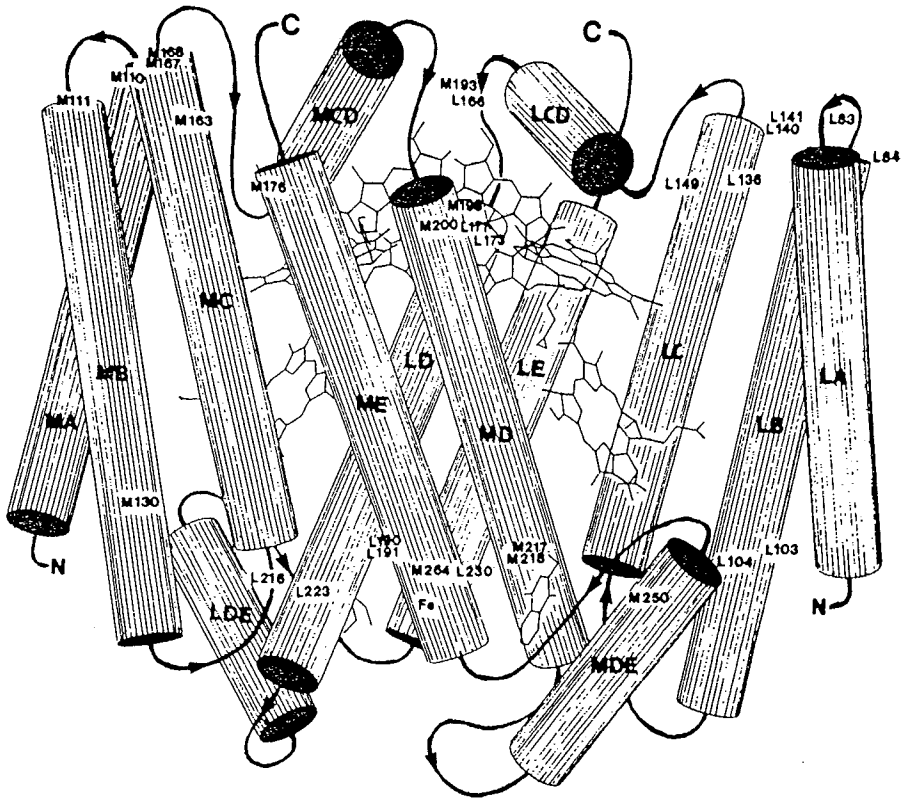

Fig. 13. Column model for the core of the reaction center from *Rps. viridis*. Only helices that are presumably conserved in photosystem II reaction centers are shown. The connections of the helices are only indicated schematically. The transmembrane helices of the L (M) subunit are labeled by LA-LE (MA-ME) and the major helices in the connections by LCD (MCD) and LDE (MDE). P's are at the interface of the L and M subunits between the D and E helices, and the BP's are near the L helices. The binding site for Q_A is between the LDE and LD helices. The location of the amino acids conserved between all L and M subunits and the D1 and D2 proteins, as well as those forming the quinone binding sites, is indicated by their sequence numbers (*42*).

(A) SIDE VIEW

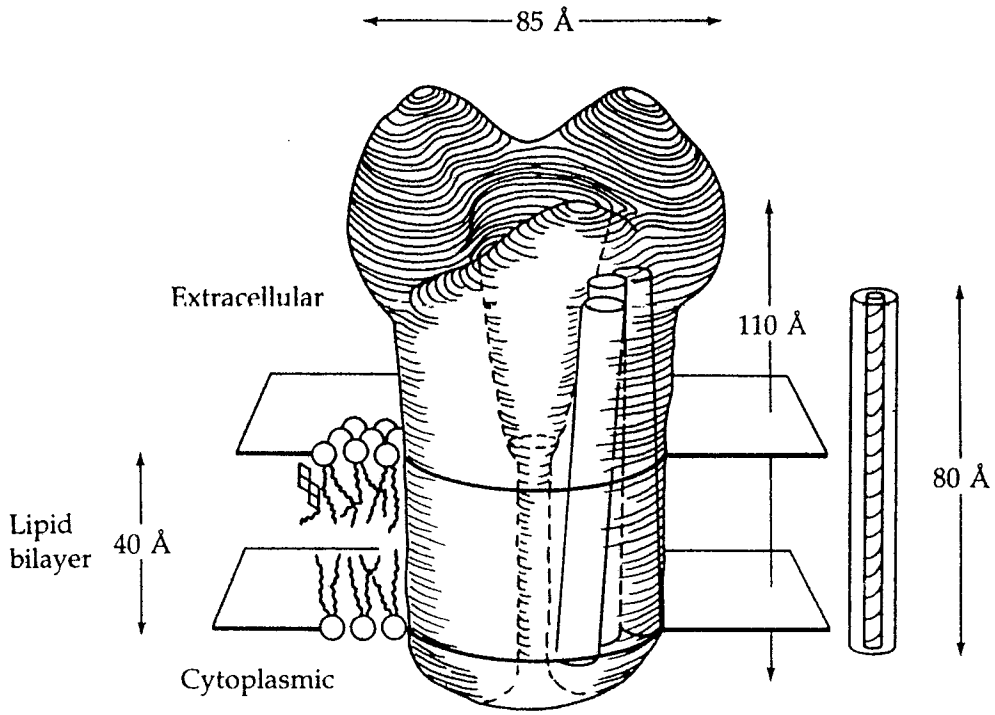

(B) FACE VIEW

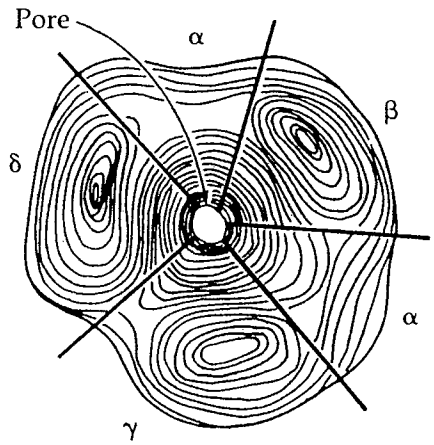

3 ACETYLCHOLINE RECEPTOR MOLECULE

Two reconstructions of the vertebrate nicotinic AChR, based on a combination of electron microscopy and x-ray diffraction. (A) Receptor molecule in lipid bilayer showing extensive protrusion into the extracellular space. Cylinders indicate dimensions of presumed α-helical portions of the peptide chains. (B) The five subunits are tentatively identified with a pore formed between them. [From Kistler et al., 1982.]

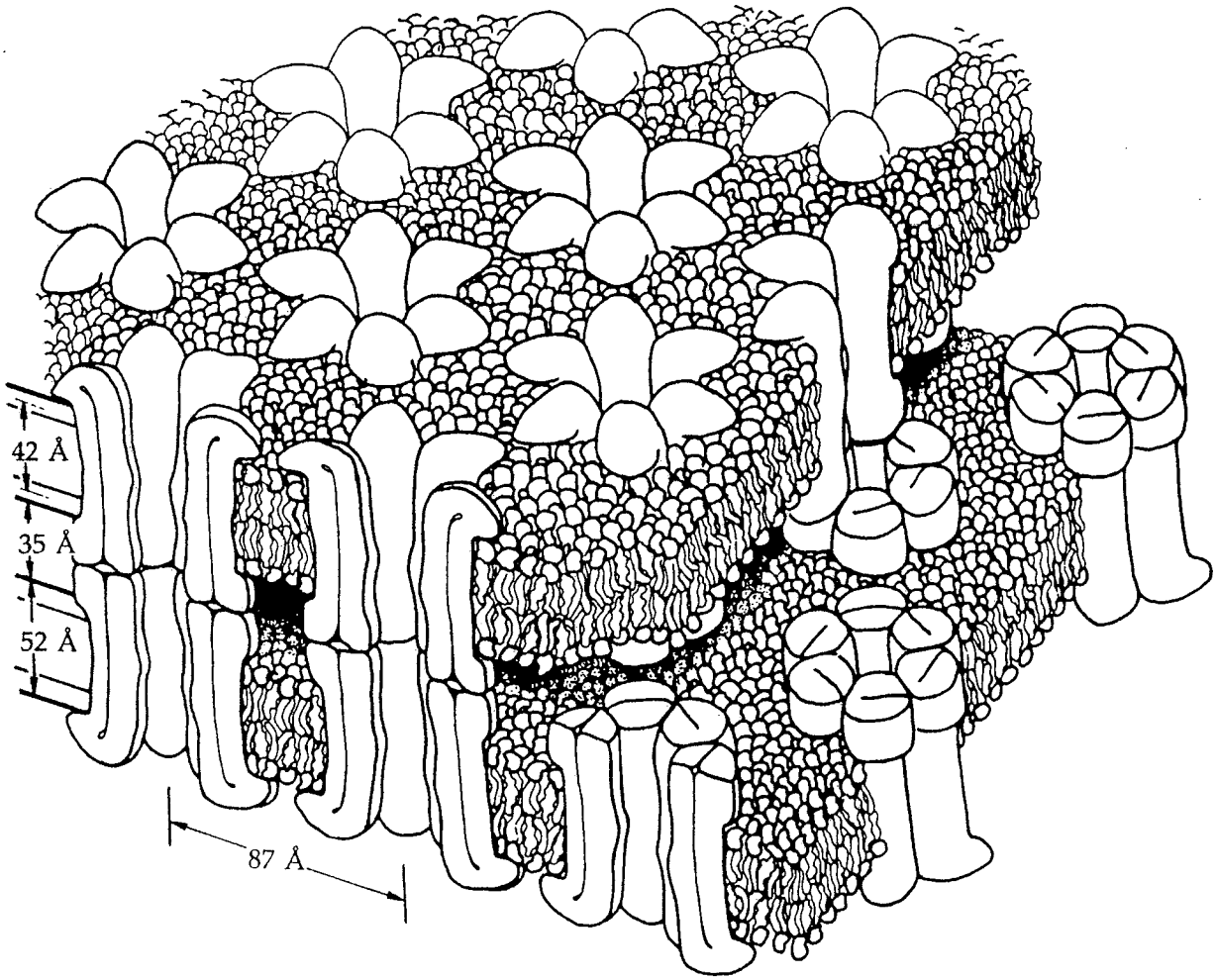

4 GAP JUNCTION CHANNELS

Connexons in the closely apposed lipid bilayers of two cells. Six connexin subunits from each cell join to make a wide aqueous pore connecting their cytoplasmic compartments. Reconstructed from electron microscope and x-ray diffraction images. [From Makowski et al., 1977.]

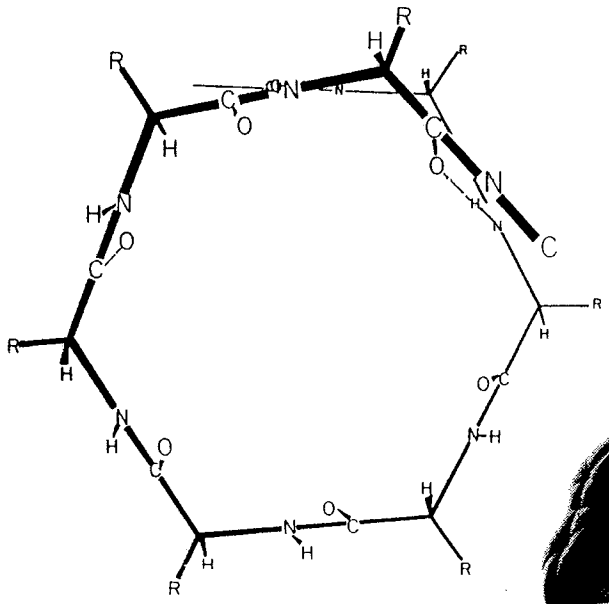

SKELETON OF π(L,D) HELIX

SPACE-FILLING MODEL

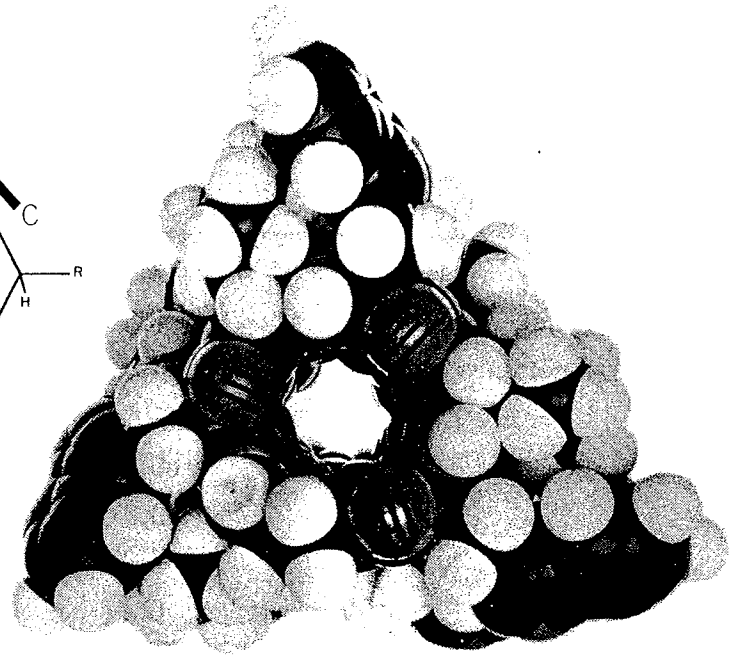

7 HELICAL STRUCTURE OF GRAMICIDIN A PORE

Proposed π(L,D) helix of gramicidin A in a membrane viewed down the axis of the helical pore. With an alternating L,D peptide, this helical structure permits hydrogen bonds between C—O and NH_2 groups six residues apart, with these polar groups lining a central pore of 4 Å diameter and the side-chain groups pointing away from the pore into the membrane. In gramicidin A none of the side chains are polar. [From Urry, 1971.]

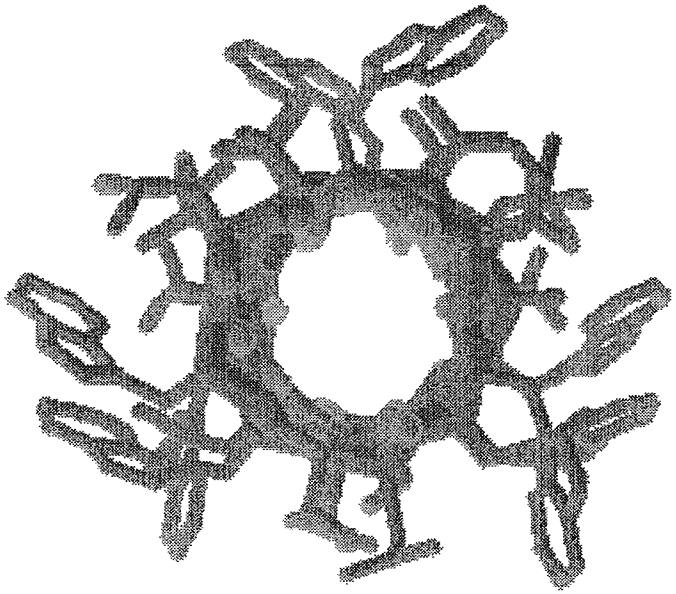

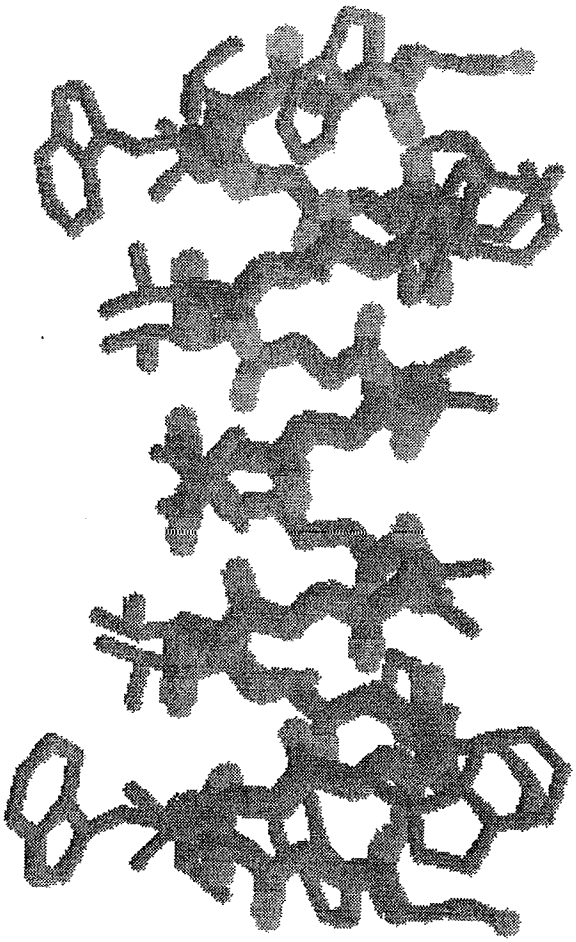

Three rotations of the SERCA1a crystal structure

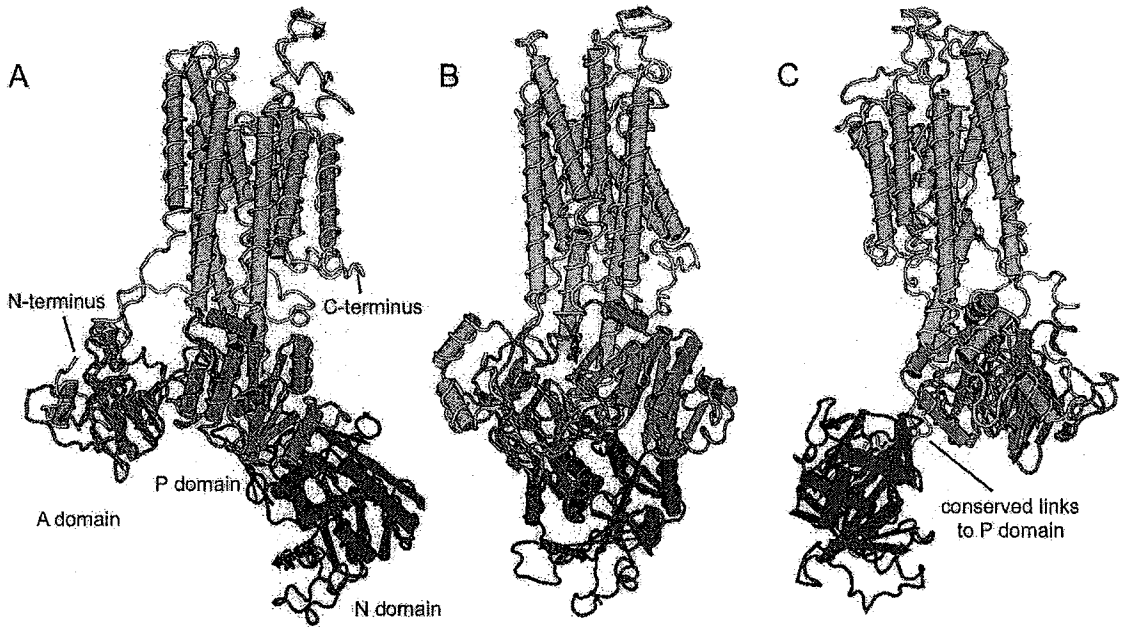

Source:

Kathleen J. SWEADNER and Claudia DONNET (2001)
Structural similarities of Na,K-ATPase and SERCA, the Ca^{2+}-ATPase of the sarcoplasmic reticulum. Biochem. J. 356:685–704. (review)

Examples of ion transporters on the plasma membrane

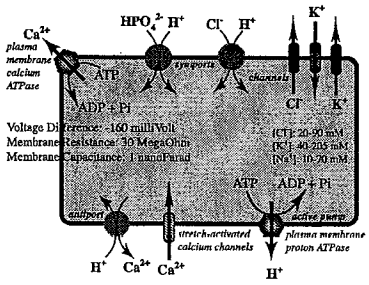

proton-motive force:

$$\Delta\mu_{H^+} = \Delta\Psi - \frac{RT}{F} \bullet \ln \frac{a_{out}^{H^+}}{a_{in}^{H^+}}$$

Three dimensional structure of a P-type active pump

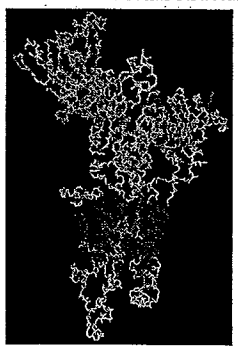

"The structure of the SERCA1 from rabbit has been solved. The structure was published in Nature: Toyoshima, C., Nakasako, M., Nomura, H., and Ogawa, H. (2000) Crystal structure of the calcium pump of sarcoplasmic reticulum at 2.6 Å resolution. Nature 405:647-655. The structure can also be found at the PDB databank with the accession number 1EUL.

The structure seen here was made with Swiss PDB-viewer which can be downloaded from the ExPASy site.

TM regions are red, conserved segments are yellow, universally conserved residues are violet, and calcium coordinating residues are green. The two calcium ions are seen as violet spheres.

When time permits it is my plan to incorporate as much as possible of the structural information in the alignments of the different subfamilies of P-type ATPases.

Last updated the : 4-8-2000 by Kristian B. Axelsen."

SOURCE:
http://biobase.dk/%7Eaxe/structure.html

Three dimensional structure of a P-type active pump: schematic view

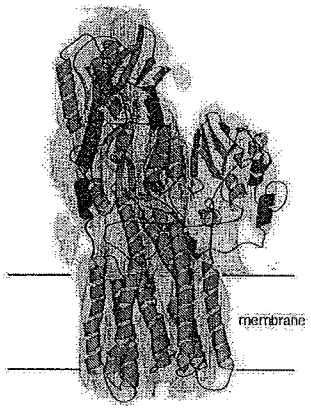

In the patch clamp technique, a small micropipette is appressed to the cell membrane. A high resistance seal forms between the membrane and the micropipette glass. With appropriate electronics (a current to voltage converter operating at very high amplification), it is possible to visualize the opening and closing of individual channels in the membrane. The currents from individual channels are in the range of picoAmperes[1].

From the front cover of the March 1992 Scientific American issue in which the 1991 Nobel Prize Laureates Erwin Neher and Bert Sakmann described the patch clamp technique.

[1] Hamill OP, ME Neher, B Sakmann, FJ Sigworth (1981)Improved patch clamp techniques for high-resolution recording from cells and cell-free membrane patches. Pflugers Archiv 391:85-100.

An example of patch clamp measurements on a protoplast.

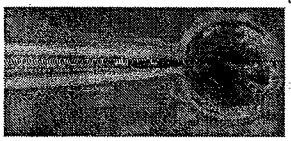

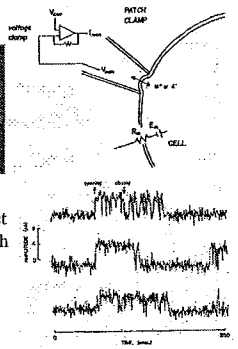

The micropipette is appressed against the protoplast membrane. With a high gain current-voltage amplifier, it is possible to observe channel opening and closing events.

Here is one example of patch clamp experiments: stretch-activated Ca^{2+} channels. The channels can be inhibited by gadolinium. In 'fungal cells', if the stretch-activated Ca^{2+} channels are inhibited, hyphal growth stops: irreversibly in *Saprolegnia ferax*[1], transiently in *Neurospora crassa*[2].

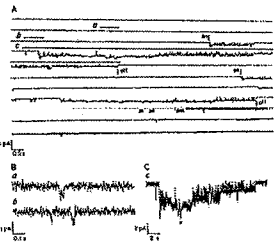

Example of stretch-activated (SA) Ca^{2+} channel activity in *Saprolegnia ferax*[3].

[1] Garrill A, SL Jackson, RR Lew, IB Heath (1993) Ion channel activity and tip growth: tip-localized stretch-activated channels generate an essential Ca^{2+} gradient in the oomycete *Saprolegnia ferax*. Eur. J. Cell Biol. 60:358-365.
[2] Levina, NN, RR Lew, GJ Hyde, IB Heath (1995) The roles of calcium ions and plasma membrane ion channels in hyphal tip growth of *Neurospora crassa*. J. Cell Sci. 108:3405-3417.
[3] Levina, NN, RR Lew, IB Heath (1994) J. Cell Sci. 107:127-134.

74

Science 280: 69-77 (1998) [98192802]

The structure of the potassium channel: molecular basis of K+ conduction and selectivity.

DA Doyle, J Morais Cabral, RA Pfuetzner, A Kuo, J M Gulbis, S L Cohen, BT Chait & R MacKinnon

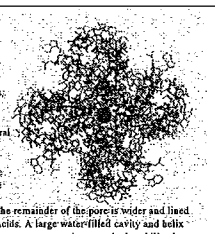

The potassium channel from Streptomyces lividans is an integral membrane protein with sequence similarity to all known K+ channels, particularly in the pore region. X-ray analysis with data to 3.2 angstroms reveals that four identical subunits create an inverted teepee, or cone, cradling the selectivity filter of the pore in its outer end. The narrow selectivity filter is only 12 angstroms long, whereas the remainder of the pore is wider and lined with hydrophobic amino acids. A large water-filled cavity and helix dipoles are positioned so as to overcome electrostatic destabilization of an ion in the pore at the center of the bilayer. Main chain carbonyl oxygen atoms from the K+ channel signature sequence line the selectivity filter, which is held open by structural constraints to coordinate K+ ions but not smaller Na+ ions. The selectivity filter contains two K+ ions about 7.5 angstroms apart. This configuration promotes ion conduction by exploiting electrostatic repulsive forces to overcome attractive forces between K+ ions and the selectivity filter. The architecture of the pore establishes the physical principles underlying selective K+ conduction.

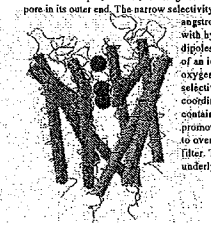

Three dimensional structure of a chloride channel

http://tcdb.ucsd.edu/tcdb/tcfamilybrowse.php?tcname=2.A.4

Transport Protein Database

The Saier Laboratory Bioinformatics Group

2.A.4 The Cation Diffusion Facilitator (CDF) Family

The CDF family is a ubiquitous family, members of which are found in bacteria, archaea and eukaryotes. They transport heavy metals including cobalt, cadmium and zinc. All members of the CDF family possess six putative transmembrane spanners. These proteins exhibit an unusual degree of sequence divergence and size variation (300-750 residues). Eukaryotic proteins exhibit differences in cell localization and polarity. Thus, some catalyze heavy metal uptake while others catalyze efflux, and some are found in plasma membranes while others are in organellar membranes. Prokaryotic and eukaryotic proteins cluster separately. The mechanisms of energy coupling are not well understood, but these proteins are secondary carriers which utilize the pmf and therefore probably function by H^+ antiport (for metal efflux) or H^+ symport (for metal uptake).

The generalized transport reaction for CDF family members is:

Me^{2+} (in or out) pmf Me^{2+} (out or in).

References:

Li, L. and J. Kaplan (2001). The yeast gene MSC2, a member of the cation diffusion facilitator family, affects the cellular distribution of zinc. J. Biol. Chem. 276: 5036-5043.

Nies, D.H. and S. Silver (1995). Ion efflux systems involved in bacterial metal resistances. J. Industr. Microbiol. 14: 186-199.

Paulsen, I.T. and M.H. Saier, Jr. (1997). A novel family of ubiquitous heavy metal ion transport proteins. J. Membr. Biol. 156: 99-103.

Xiong, A. and R.K. Jayaswal (1998). Molecular characterization of a chromosomal determinant conferring resistance to zinc and cobalt ions in *Staphylococcus aureus*. J. Bacteriol. 180: 4024-4029.

Examples:

TC#	Name	Organismal Type	Example
2.A.4.1.1	Cd^{2+} Zn^{2+}, Co^{2+} efflux permease	Bacteria	CnrD of *Alcaligenes eutrophus*
2.A.4.1.2	Zn^{2+}, Co^{2+} efflux permease	Bacteria	ZntA of *Staphylococcus aureus*
2.A.4.1.1	Mitochondrial Co^{2+}/Zn^{2+} uptake permease	Yeast	Cot1 of *Saccharomyces cerevisiae*
2.A.4.2.2	Mitochondrial Zn^{2+}, Cd^{2+} uptake permease	Yeast	ZrcP of *Saccharomyces cerevisiae*
2.A.4.2.3	Plasma membrane Zn^{2+} efflux permease	Animals	Znt1 of *Rattus norvegicus*
2.A.4.3.1	Vesicular Zn^{2+} uptake permease	Animals	Znt3 of *Rattus norvegicus*
2.A.4.4.1	Nuclear/ER Zn^{2+} uptake permease	Yeast	MSC2 of *Saccharomyces cerevisiae*

Bioessays **22:** 227-234 (2000) [20148385]

Common structural features in gramicidin and other ion channels.

B. A. Wallace

Department of Crystallography, Birkbeck College, University of London, London WC1E 7HX, UK.
ubcg91c@ccs.bbk.ac.uk

This review compares and contrasts the structures of several different types of ion channels with known three-dimensional structures, including gramicidin and the family of peptaibol channels, as well as the Streptomyces lividans potassium channel, to reveal common features in their structures that relate to their functional roles in ion binding and transport across membranes. Specifically, the locations of aromatic amino acids, the dimensions of the molecules, the multimeric nature of the channels and the roles of hydrogen bonds in stabilising such structures, the means by which the channels open and close, and the chemical nature of the groups which make up the channel lumen are discussed. The emphasis is on the commonality of features found in model channels, which may ultimately be found in other biological channel structures.